ELSEVIER

Ecological Modelling 80 (1995) 205–235

ECOLOGICAL MODELLING

Coupling biochemical and biophysical processes at the leaf level: an equilibrium photosynthesis model for leaves of C_3 plants

Nedialko T. Nikolov *, William J. Massman, Anna W. Schoettle

USDA FS / Rocky Mountain Forest and Range Experiment Station, 240 West Prospect Road, Fort Collins, CO 80526, USA

Received 29 November 1993; accepted 12 April 1994

Abstract

The paper presents a generic computer model for estimating short-term steady-state fluxes of CO_2, water vapor, and heat from broad leaves and needle-leaved coniferous shoots of C_3 plant species. The model explicitly couples all major processes and feedbacks known to impact leaf biochemistry and biophysics including biochemical reactions, stomatal function, and leaf-boundary layer heat- and mass-transport mechanisms. The ability of the model to successfully predict measured photosynthesis and stomatal-conductance data as well as to simulate a variety of observed leaf responses is demonstrated. A model application investigating physiological and environmental regulation of leaf water-use efficiency (WUE) under steady-state conditions is discussed. Simulation results suggest that leaf physiology has a significant control over the environmental sensitivity of leaf WUE. The implementation of a highly efficient solution technique allows the model to be directly incorporated into plant-canopy and terrestrial ecosystem models.

Keywords: Carbon; Temperature; Water dynamics

1. Introduction

Leaf CO_2 fixation and heat exchange are fundamental processes to the carbon and water budges of terrestrial ecosystems from an individual-plant level to a global scale. Thus, stomatal conductance has been found to exert a direct control over the regional atmospheric circulation and climate (Avissar and Pielke, 1991). It is now recognized that a robust simulation of leaf ecophysiological responses is critical for predicting ecosystem flows of carbon, water and nutrients, as well as for modelling efforts aimed at coupling terrestrial ecosystems with atmospheric dynamics (Pielke et al., 1993). On the other hand, detailed studies reveal a complex pattern of interactions between the physical environment and leaf physiological and morphological properties that cannot be described by simple empirical relationships. Hence, mechanistic models of leaf responses may be needed that combine algorithmic complexity with a computational efficiency.

During the past 20 years, a large body of knowledge and experimental data has been accumulated about leaf biochemistry and stomatal

* Corresponding author.

SSDI 0304-3800(94)00072-P

function of C_3 plants (e.g. Sharkey, 1985a,b; Zeiger et al., 1987; Woodrow and Berry, 1988). Mathematical models have been developed for many aspects of the leaf C_3 physiology (e.g. Jarvis, 1976; Farquhar et al., 1980; Farquhar and von Caemmerer, 1982; Farquhar and Wong, 1984; Brooks and Farquhar, 1985; Givnish, 1986; Ball et al., 1987; Massman and Kaufmann, 1991). A number of studies have emphasized the importance of feedbacks between biochemical and biophysical processes for an adequate understanding of leaf responses. Several researchers have incorporated such feedbacks into simulation models and made successful predictions of observed photosynthetic rates and stomatal conductances (e.g. Ball, 1988; Leuning, 1990; Collatz et al., 1991; Friend, 1991; Harley and Tenhunen, 1991; Harley et al., 1992). However, none of the published models provides a thorough description of the leaf system. We present in this paper a generic steady-state flux model (LEAFC3) that couples in a mechanistically explicit way the leaf's major biochemical processes with stomatal function and the energy- and mass-exchange mechanisms in the leaf-boundary layer. The model implements a concept similar to one employed by Ball (1988) and Collatz et al. (1991) but incorporates the full spectrum of important processes and interactions (including feedbacks between stomatal and leaf-boundary layer mechanisms and the effect of leaf wetness status on biophysical responses) and uses a different highly optimized solution technique. Our goal was to develop an algorithm that has a sufficient level of detail to simulate complex leaf–environmental interactions over a broad range of conditions, yet enough computational efficiency to be directly incorporated into plant-canopy models. This practical objective guided our decision to provide a comprehensive discussion of all the mathematical details necessary to evaluate the model. To facilitate model implementation by other researchers, we have included its computer code in the appendix.

2. Model description

Leaf responses are determined by the interaction between biochemical reactions, mass transfer through stomates and the leaf-boundary layer, and radiative exchange.

2.1. Leaf biochemical processes

This part of the model implements concepts and mechanisms discussed by Farquhar et al. (1980), Farquhar and von Caemmerer (1982), Farquhar and Wong (1984), Sharkey (1985a), Brooks and Farquhar (1985), Farquhar (1988), Collatz et al. (1991), and Harley et al. (1992).

The net CO_2 assimilation rate (A_n, μmol CO_2 m^{-2} s^{-1}) of a leaf is given by

$$A_n = A - R_d \tag{1}$$

where A is the gross rate of CO_2 uptake and R_d is the dark respiration, i.e. the CO_2 evolution resulting from processes other than photorespiration. Gross photosynthesis is defined as the most limiting of three potential rates, i.e.

$$A = \min\{W_c, W_j, W_p\} \tag{2}$$

where W_c is the assimilation rate constrained by the activation and kinetic properties of the Rubisco enzyme alone, W_j is the rate limited solely by the regeneration capacity of ribulose bisphosphate (RuBP), i.e. the enzyme substrate, and W_p is the capacity for utilization of the products of photosynthesis (i.e. the rate of sucrose and starch synthesis from triose phosphate produced in the Calvin cycle).

Because the transition from one limitation to another appears to be somewhat gradual in reality, it is more appropriate to estimate A from the following quadratic equations rather, than from Eq. 2 (Collatz et al., 1991):

$$\beta A^2 - (A_e + W_p)A + A_e W_p = 0 \tag{3}$$

$$\alpha A_e^2 - (W_c + W_j)A_e + W_c W_j = 0 \tag{4}$$

Here, A_e is an intermediate gross rate of CO_2 assimilation which represents the minimum of W_c and W_j, and α and β are convexity coefficients defining the smoothness of the transition (the closer to unity the coefficients are the sharper the transition). In this model, $\alpha = 0.95$ and $\beta = 0.97$.

The Rubisco limited rate of photosynthesis is given by:

$$W_c = \frac{V_{cmax}(C_i - \Gamma)}{C_i + K_c(1 + O/K_o)} \tag{5}$$

where V_{cmax} is the maximum rate of carboxylation (μmol m^{-2} s^{-1}) at 21% ambient oxygen concentration, C_i and O are the CO_2 and O_2 partial pressures (Pa) in the intercellular air space of the leaf, Γ is the CO_2 compensation point (Pa) in the absence of dark respiration, K_c and K_o are Michaelis–Menten kinetic parameters (Pa) for CO_2 and O_2, respectively.

The RuBP regeneration is controlled by the rate of electron transport/photo-phosphorylation. Assuming that pseudocyclic electron transport is typically involved in the adenosine triphosphate production, the corresponding assimilation rate is

$$W_j = \frac{J(C_i - \Gamma)}{4.5(C_i + 2.33\Gamma)} \tag{6}$$

where J is the potential rate of whole-chain electron transport (μmol m^{-2} s^{-1}).

Collatz et al. (1991) defined the gross assimilation rate limited by the triose phosphate utilization as:

$$W_p = \frac{V_{cmax}}{2} \tag{7}$$

Based on findings by Sharkey (1985a), Harley et al. (1992) derived a more elaborate formulation for W_p. We use Eq. 7 for its simplicity and because photosynthesis is not normally constrained by W_p. When this limitation takes place, net assimilation becomes insensitive to short-term changes in CO_2 and O_2 partial pressures. Such a response can occur in severely water-stressed leaves, leaves at low temperatures, or in leaves exposed to high levels of CO_2 and light intensity (Sharkey, 1985b).

The CO_2 compensation point depends on O_2 partial pressure and the Rubisco specificity (a ratio of the kinetic parameters K_o and K_c), τ:

$$\Gamma = 0.5\frac{O}{\tau} \tag{8}$$

Since both K_c and K_o are functions of temperature (Eqs. 14 and 15), τ has a temperature sensitivity as well. We used the second-order polynomial given by Brooks and Farquhar (1985) to derive a computationally efficient expression for Γ, i.e.

$$\Gamma = O\left[213.88 \times 10^{-6} + 8.995 \times 10^{-6}(T_l - 25) + 1.772 \times 10^{-7}(T_l - 25)^2\right] \tag{9}$$

where T_l is the leaf temperature in °C. Eq. 9 produces almost identical results with Eq. 8 as parameterized by Harley et al. (1992).

The potential rate of electron transport (J) is constrained by incident photosynthetic photon flux density (PPFD) and leaf temperature. The switch of control over J between PPFD and temperature is approximated by a quadratic equation similar to Eqs. 3 and 4, i.e.

$$J = \frac{(J_{max} + \varphi Q) - \sqrt{(J_{max} + \varphi Q)^2 - 4\theta\varphi Q J_{max}}}{2\theta} \tag{10}$$

where θ is a convexity coefficient (between 0.7 and 0.9 for C_3 plants; in this model $\theta = 0.8$), J_{max} is the light-saturated potential rate of electron transport, Q is the intensity of incident PPFD (both Q and J_{max} are in μmol m^{-2} s^{-1}), and φ is the efficiency of energy conversion for electron transport. The latter is defined as

$$\varphi = a\frac{(1-f)}{2} \tag{11}$$

where a is the leaf absorption coefficient for PPFD (about 0.85 for green leaves) and f is an energy loss factor (i.e. the fraction of absorbed PPFD unavailable for photosynthesis). The f parameter is species-specific and typically ranges from 0.05 to 0.5 (Ziegler-Jöns and Selinger, 1987). Eq. 10 implies that, under low irradiance, RuBP regeneration becomes insensitive to temperature.

The maximum rate of potential electron transport, J_{max} is controlled by leaf temperature (Farquhar, 1988), i.e.

$$J_{max} = J_{m25}\frac{\exp\left[(3.3621 \times 10^{-3}T_{lk} - 1)E/(RT_{lk})\right]}{1 + \exp\left[(ST_{lk} - H)/(RT_{lk})\right]} \tag{12}$$

where J_{m25} is the rate of J_{max} at 25° C, T_{lk} is the leaf temperature in K, R is the universal gas

constant (8.3143 J mol^{-1} K^{-1}), E is an activation energy of the reaction (81993 J/mol), and S and H are parameters related to the reaction's enthalpy (711.36 J mol^{-1} K^{-1} and 219814 J/mol, respectively). Values for E, S and H were estimated from data for cotton presented by Harley et al. (1992). Eq. 12 has a temperature optimum at 33.98° C.

The temperature dependency of V_{cmax} is given by

$$V_{cmax} = V_{m25}\frac{\exp[46.9411 - 116300/(RT_{lk})]}{1 + \exp[(650T_{lk} - 202900)/(RT_{lk})]} \quad (13)$$

where V_{m25} is the rate of V_{cmax} at 25° C. The parameters J_{m25} and V_{m25} depend primarily upon species physiology but can be also influenced by the leaf age (Fields, 1983; Schoettle, 1990) and prevailing growth conditions in terms of temperature (Berry and Björkmann, 1980), atmospheric CO_2 concentration (Delucia et al., 1985; Besford, 1990; Harley et al., 1992) or availability of light, water, and mineral nitrogen (Wong et al., 1985a,b; Evans, 1989; Leuning et al., 1991). The kinetic parameters for CO_2 and O_2 are calculated from

$$K_c = PK_{c25}\exp[32.462 - 80470/(RT_{lk})] \quad (14)$$

$$K_o = PK_{o25}\exp[5.854 - 14510/(RT_{lk})] \quad (15)$$

where P is the total atmospheric pressure (Pa), and K_{c25} and K_{o25} are the corresponding parameter values at 25° C (mol/mol). The latter do vary with species, but typical values for C_3 plants are $K_{c25} = 27 \times 10^{-5}$ mol/mol and $K_{o25} = 40 \times 10^{-2}$ mol/mol (Woodrow and Berry, 1988). Eqs. 13, 14, and 15 are derived from expressions given by Harley et al. (1992).

Dark respiration R_d (μmol CO_2 m^{-2} s^{-1}) rises exponentially with temperature and is assumed to be proportional to the maximum carboxylation velocity at 25° C, i.e.

$$R_d = c_{dr}V_{m25}\exp[34.07 - 84450/(RT_{lk})] \quad (16)$$

The coefficient c_{dr} is expected to vary to some extent with ambient CO_2 concentration (Harley and Tenhunen, 1991; Amthor et al., 1992; Wullschleger and Norby, 1992; Idso and Kimball, 1993) and, perhaps, plant species. In this model, we use as a default the value suggested by Collatz et al. (1991), i.e. $c_{dr} = 0.015$. To account for an observed inhibition of dark respiration in actively-photosynthesizing leaves (e.g. Peisker et al., 1981; Brooks and Farquhar, 1985), R_d is linearly increased up to 67% above the value calculated by Eq. 16 when PPFD < 50 μmol m^{-2} s^{-1}. The actual mechanisms causing the R_d suppression in the light, and the magnitude of the reduction are still unknown. However, most studies agree that the inhibition is between 12% and 70% and depends on yet poorly understood ontogenic and physiological factors (e.g. Azcon-Bieto et al., 1981; Peisker et al., 1981; Sharp et al., 1984; Brooks and Farquhar, 1985; Kent et al., 1992).

The intercellular CO_2 concentration (c_i) depends on the net rate of CO_2 uptake and the physiologic and boundary-layer resistances at the leaf surface. From the relationship between net assimilation and leaf conductance (e.g. Von Caemmerer and Farquhar, 1981), ignoring the minute effect of transpiration on the CO_2 influx, it follows that

$$c_i = c_a - A_n\frac{1.6g_{bv} + 1.37g_{sv}}{g_{sv}g_{bv}} \quad (17)$$

where c_a is the CO_2 concentration in the ambient air (both c_i and c_a have units of mol/mol), g_{sv} and g_{bv} are the leaf stomatal and boundary-layer conductances to water vapor (μmol m^{-2} s^{-1}), respectively. The coefficient 1.6 is a ratio of the molecular diffusivities of water vapor and CO_2 in still air. This ratio reduces to 1.37 (i.e. $1.6^{2/3}$) in the leaf boundary layer due to the effect of air flow. To estimate intercellular CO_2 partial pressure (C_i) one needs to multiply c_i by the total pressure (P).

2.2. Stomatal conductance

Ball et al. (1987) and Ball (1988) proposed a semi-empirical equilibrium model of stomatal conductance based on a number of gas exchange experiments with C_3 and C_4 plants, i.e.

$$g_{sv} = mA_n\frac{h_b}{c_b} + b_{sv} \quad (18)$$

In this equation, m is a species-specific non-dimensional parameter that determines the com-

posite sensitivity of g_{sv} to net CO_2 assimilation (A_n), and relative humidity (h_b) and CO_2 concentration (c_b) at the leaf surface, i.e. within the leaf boundary layer (h_b is a decimal fraction, and c_b is a mole fraction). For C_3 plants, m varies between 8 and 16 (Ball, 1988). The free parameter b_{sv} is the stomatal conductance that remains unaffected by the atmospheric environment or leaf biochemistry. Usually, it is a small number, e.g. for C_3 plants $b_{sv} \approx 0.01$ mol m^{-2} s^{-1} (Ball, 1988; Collatz et al., 1991). A thorough discussion of the experimental design and the rationale that have led to the development of this stomatal model is provided by Ball (1988).

The relationship in Eq. 18 has been confirmed under steady-state conditions by independent investigators for a variety of plant species (Grantz, 1990; Leuning, 1990; Harley et al., 1992; Thompson and Wheeler, 1992; Dougherty et al., 1994). Several modifications of Eq. 18 have been proposed that fit the data measured for particular species better than the original model (e.g. Leuning, 1990; Lloyd, 1991; Aphalo and Jarvis, 1993a; Dougherty et al., 1994). In the absence of a clear understanding about the appropriate general form of the photosynthesis–stomatal relationship, we decided to use Eq. 18 for its simplicity and because it appears to explain above 70% of the observed variation in most data sets. Although it does not provide a truly mechanistic explanation of stomatal behavior, Eq. 18 implies that (i) stomatal conductance and photosynthesis are linked and cannot be predicted independently; (ii) stomates respond to the CO_2 and humidity levels of their immediate environment, the leaf boundary layer (Bunce, 1985) or perhaps the substomatal cavity, and do not directly sense ambient atmospheric conditions; and (iii) carbon gain and water loss of plants can be substantially influenced by factors affecting leaf boundary-layer thickness such as wind speed and leaf geometry.

To simulate the effect of leaf water deficit on stomatal conductance and net photosynthesis, we substituted the following expression for m in Eq. 18

$$M = m/\left[1 + (\Psi/\Psi_{crit})^n\right]$$

where Ψ is current leaf water potential ($-$MPa), Ψ_{crit} is the water potential at which stomatal conductance is reduced by 50% of its unstressed level, and n is a fitting parameter (usually between 3 and 7) defining the steepness of the curve when $\Psi \approx \Psi_{crit}$. This sigmoid function has been found to describe accurately the detrimental effect of falling water potential on stomatal conductance (Fisher et al., 1981; Landsberg, 1986) and photosynthesis (Deng et al., 1990).

Because leaf-boundary layer resistance is always greater than zero, one can typically expect that, near the leaf surface, relative humidity is higher and CO_2 concentration is lower than in the ambient air. Thus, an accurate estimation of h_b and c_b appears to be important for prediction of g_{sv}. Assuming a balance of the fluxes of water vapor and CO_2 between the leaf surface and the top of the leaf boundary layer, it can be shown for a dry leaf surface that

$$h_b = \frac{g_{sv}e_i + g_{bv}e_a}{e_s(T_l)(g_{sv} + g_{bv})} \tag{19}$$

and

$$c_b = \frac{1.6g_{bv}c_a + 1.37g_{sv}c_i}{1.6g_{bv} + 1.37g_{sv}} = c_a - A_n\frac{1.37}{g_{bv}} \tag{20}$$

where e_i is the water-vapor pressure in the intercellular air space of the leaf, $e_s(T_l)$ is the saturation vapor pressure at leaf temperature (Eq. 38 or 39), and e_a is the vapor pressure in the ambient air (all e_i, $e_s(T_l)$ and e_a are in Pa). Eq. 19 implies that the air inside the leaf boundary layer is at leaf temperature. In the case of a wet leaf, Eq. 20 still holds (assuming that the CO_2 exchange through stomatal pores is not significantly affected by water droplets residing on the leaf surface), but then Eq. 19 does not apply because the air next to a wet surface is normally vapor-saturated and, therefore, $h_b = 1$.

The water-vapor pressure inside the leaf is related to the saturation vapor pressure at leaf temperature and the leaf water potential (Ψ) by the thermodynamic expression (e.g. Ball, 1987)

$$e_i = e_s(T_l)\exp\left[18\Psi/(RT_{lk})\right]$$

This relationship produces approximately 0.7% reduction in e_i per 1.0 MPa water potential. Because a leaf water potential below −5.0 MPa is lethal for most plant species (Hinckley et al., 1978,1983), the actual intercellular vapor pressure can be expected to deviate from saturation at most by 3.5%. This amounts to a change in leaf-surface relative humidity (h_b) of less than 1.5% according to Eq. 19. Since such an error is rather small compared to the uncertainty associated with g_{bv} estimates, in the model we substituted e_i for $e_s(T_l)$.

2.3. Leaf-boundary layer conductance

The non-dimensional groups provide a handy tool for quantifying the leaf boundary layer. A comprehensive discussion of this approach can be found in publications by Campbell (1977), Gates (1980), and Monteith and Unsworth (1990).

The all-sided leaf-boundary layer conductance to water vapor (m/s) is given by

$$g_{bv} = \frac{D_v S_h}{d} \tag{21}$$

where d is the characteristic dimension of a leaf (m) or, in practical terms, the leaf width for broad leaves, and the needle diameter for conifers. D_v is the molecular diffusivity of water vapor in air (m^2/s). It is a function of absolute air temperature, T_{ak} (K) and barometric pressure, P (Pa) (Smithsonian Meteorological Tables), i.e.

$$D_v = 8.7941 \times 10^{-5} \frac{T_{ak}^{1.81}}{P} \tag{22}$$

The parameter S_h is the Sherwood number. It is related to the Nusselt number (N_u) by

$$S_h = 0.962 N_u \tag{23}$$

In the case of a forced convection (and assuming a laminar air flow over the leaf surface), the Nusselt number is estimated for broad leaves from (Gates, 1980)

$$N_u = 1.18 P_r^{0.33} R_e^{0.5} \tag{24}$$

For coniferous shoots, under the same conditions, and assuming cylindric needles, N_u is given by

$$N_u = \frac{0.69 P_r^{0.33} R_e^{0.5}}{2.1} \tag{25}$$

In the equations above, P_r is the Prandtl number defined as a ratio of the kinematic viscosity to the thermal diffusivity of the fluid (for air, $P_r = 0.72$), and R_e is the Reynolds number. The constant 2.1 in Eq. 25 is an average shelter factor proposed by Grant (1984) and accounts for the mutual interference between the needles on a shoot inside an air flow. The Reynolds number is a function of the kinematic viscosity of dry air, ν (m^2/s) and the wind velocity, u (m/s), i.e.

$$R_e = \frac{du}{\nu} \tag{26}$$

Kinematic viscosity of air is a ratio of the dynamic viscosity, μ (kg m^{-1} s^{-1}) to the density of dry air, ρ (kg/m^3) which are estimated from (Smithsonian Meteorological Tables)

$$\mu = 1.4963 \times 10^{-6} \frac{T_{ak}^{1.5}}{(T_{ak} + 120)} \tag{27}$$

and

$$\rho = 3.4838 \times 10^{-3} \frac{P}{T_{ak}} \tag{28}$$

Combining Eqs. 21 through 28 yields the following expression for the forced-convective leaf boundary-layer conductance (g_{bvf}) in m/s:

$$g_{bvf} = c_f T_{ak}^{0.56} \left[(T_{ak} + 120) \frac{u}{dP} \right]^{0.5} \tag{29}$$

where c_f equals 4.322×10^{-3} for broad leaves, and 1.2035×10^{-3} for coniferous shoots. The forced-convective leaf boundary-layer conductance has a very low temperature sensitivity, especially when expressed in mole units. For example, a temperature difference of 30° C produces a change in g_{bvf} of less than 1%. Because an error of this magnitude is much smaller than the expected accuracy of g_{bv} estimates, we compute g_{bvf} using ambient free-air temperature instead of leaf-surface temperature.

At low wind speed, the heat exchange is dominated by free convection and N_u becomes a

function of the Grashof number, G_r. In this case, N_u is calculated for broad leaves from

$$N_u = (P_r G_r)^{0.25} = 0.921 G_r^{0.25} \quad (30)$$

For coniferous shoots, we use a formula derived for horizontal cylinders (Gates, 1980; Monteith and Unsworth, 1990), i.e.

$$N_u = 0.53(P_r G_r)^{0.25} = 0.488 G_r^{0.25} \quad (31)$$

The Grashof number depends on the absolute difference in virtual temperatures between the leaf surface and the ambient air, i.e.

$$G_r = \frac{\kappa g d_o^3 |T_{vl} - T_{va}|}{\nu^2} \quad (32)$$

where T_{vl} and T_{va} are the virtual temperatures of leaf and free air (° C), respectively, κ is a coefficient of the volumetric thermal expansion of air (3.66×10^{-3} °C^{-1}), g is the acceleration due to gravity (9.81 m/s^2), and d_o is the leaf width for broad leaves, and the shoot diameter for conifers (m). In the case of conifers, shoot diameter rather than needle diameter is used in the denominator of Eq. 21 to estimating the free-convective leaf boundary-layer conductance, g_{bve}. The reason is that, in the absence of a forced air flow, the shoot behaves aerodynamically as an intact object (i.e. a cylinder) rather than as a structured collective of needles. By combining Eqs. 21 through 23 with Eqs. 30, 31 and 32, one finds for g_{bve} (m/s)

$$g_{bve} = c_e T_{lk}^{0.56} \left[\frac{T_{lk} + 120}{P} \right]^{0.5} \left[\frac{|T_{vl} - T_{va}|}{d_o} \right]^{0.25} \quad (33)$$

where $c_e = 1.6361 \times 10^{-3}$ for broad leaves, and $c_e = 0.8669 \times 10^{-3}$ for coniferous shoots. The virtual-temperature difference is calculated from (Monteith and Unsworth, 1990)

$$T_{vl} - T_{va} = \frac{T_{lk}}{1 - 0.378 e_b/P} - \frac{T_{ak}}{1 - 0.378 e_a/P} \quad (34)$$

where e_b is the water-vapor pressure inside the leaf boundary layer (Pa). For a dry leaf surface, it follows from Eq. 19 that

$$e_b = \frac{g_{sv} e_s(T_l) + g_{bve} e_a}{g_{sv} + g_{bve}} \quad (35)$$

The dependence of e_b upon g_{bve} introduces a feedback in the calculation of the free-convective leaf boundary-layer conductance. The latter is estimated using an iterative technique. In case of a wet leaf, $e_b = e_s(T_l)$. The final leaf boundary-layer conductance to water vapor (g_{bv}) is the larger of the conductances resulting from the forced and free convective exchanges.

Owing to fundamental similarity of the mechanisms for heat and mass transport, leaf boundary layer conductance to sensible heat (g_{bH}) is proportional to the water-vapor conductance, i.e.

$$g_{bH} = 0.924 g_{bv} \quad (36)$$

where the coefficient 0.924 is representative both for free and forced convection.

2.4. Leaf energy balance

In the steady-state case (i.e. when leaf temperature is constant), the total energy absorbed by a leaf is dissipated through latent and sensible heat fluxes, long-wave radiation, and metabolic storage. In mathematical terms,

$$R_i = \frac{\rho c_p}{\gamma} [e_s(T_l) - e_a] g_{tv} + \rho c_p (T_l - T_a) g_{bH} + 2\epsilon\sigma(T_l + 273.16)^4 + M_e \quad (37)$$

where R_i is the bi-directional absorbed short- and long-wave radiation (W/m^2), c_p is the specific heat of dry air (1010 J kg^{-1} K^{-1}), γ is the psychrometric constant (Pa/K), g_{tv} is the leaf total conductance for water-vapor exchange (m/s), T_a is the ambient air temperature (° C), ε is the leaf thermal emissivity (about 0.975), and σ is Stefan–Boltzmann constant (5.67×10^{-8} W m^{-2} K^{-4}). The energy stored in biochemical reactions, M_e, represents a very small fraction of R_i (i.e. ca. 0.506 J/μmol CO_2) and can be ignored. The saturation water-vapor pressure increases exponentially with temperature and can

be accurately computed over the range −9° C to 60° C from (Gueymard, 1993)

$$e_s(T_l) = 610.7\exp[17.38T_l/(T_l + 239)] \quad (38)$$

where $e_s(T_l)$ is in Pa. Eq. 38 can be approximated by a fourth-order polynomial over the temperature range from −5° C to 60° C with a maximum error of 0.48% at −2° C, i.e.

$$e_s(T_l) = 5.82436 \times 10^{-4}T_l^4 + 1.5842 \times 10^{-2}T_l^3 + 1.55186T_l^2 + 44.513596T_l + 607.919 \quad (39)$$

The use of a polynomial expression for $e_s(T_l)$, allows one to solve analytically the energy-balance equation for leaf temperature (as discussed in the next section).

The leaf total conductance to water vapor for a dry leaf surface, and the psychrometric constant are calculated from

$$g_{tv} = \frac{g_{sv}g_{bv}}{g_{sv} + g_{bv}} \quad (40)$$

and

$$\gamma = \frac{c_p P}{0.622L} \quad (41)$$

where 0.622 is a ratio of the molecular weight of water to that of dry air, and L is the latent heat of vaporization (J/kg) given by (Verstraete, 1985):

$$L = (2.50084 - 0.00234T_a) \times 10^6 \quad (42)$$

For a wet leaf, $g_{tv} = g_{bv}$. To estimate c_i, g_{sv}, and g_{tv} for broad hypostomatous leaves (i.e. with stomates occurring only on one side of the leaf), the leaf boundary layer conductance (g_{bv}) is reduced by 50% in Eqs. 17, 19, 20, and 40. Vapor conductances are converted from units of mol m^{-2} s^{-1} into m/s via multiplication by $c_{fm} = 8.309\ T_{ak}/P$.

2.5. Linking leaf processes

We have seen that net photosynthesis rate (A_n) is controlled by the leaf temperature, PPFD, and intercellular CO_2 partial pressure (C_i). However, C_i depends on A_n and stomatal conductance. The latter, in turn, is a function of A_n, and regulates, in conjunction with boundary layer conductance, the leaf temperature by constraining the partitioning of absorbed energy at the leaf surface. At low wind speed, the convective heat exchange becomes driven by differences in temperature and air density between the leaf surface and the ambient air, thus making leaf boundary-layer conductance sensitive to leaf temperature and hence to stomatal conductance. This complex pattern of feedbacks and mutual limitations requires that leaf fluxes be estimated from the simultaneous solution to a system of seven equations with seven unknowns, i.e.

$A_n = \mathbf{f}(C_i, T_l)$ Eqs. 1 through 16

$C_i = \mathbf{f}(A_n, g_{sv}, g_{bv})$ Eq. 17

$g_{sv} = \mathbf{f}(A_n, h_b, c_b)$ Eq. 18

$h_b = \mathbf{f}(g_{sv}, g_{bv}, T_l)$ Eq. 19

$c_b = \mathbf{f}(A_n, g_{bv})$ Eq. 20

$T_l = \mathbf{f}(g_{sv}, g_{bv})$ Eqs. 37 through 42

$g_{bv} = \mathbf{f}(T_l)$ Eqs. 29 and 33

Solving this system numerically can be an awkward task that involves a complex algorithm with numerous partial derivatives and time-intensive nested iterations. We will show, however, that, through certain algebraic manipulations, one can avoid the use of derivatives, eliminate most iterations, and significantly speed up model execution.

We begin with optimization of the leaf-temperature algorithm. Paw U (1987) proposed a simple method to the exact solution of the energy balance equation. If $e_s(T_l)$ in Eq. 37 is substituted for the polynomial from Eq. 39, the energy-budget expression can be rearranged in the form of a quartic equation for T_l, i.e.

$$T_l^4 + a_t T_l^3 + b_t T_l^2 + c_t T_l + d_t = 0 \quad (43)$$

where the coefficients are given by

$$a_t = (8\epsilon\sigma 273.16 + 1.5842 \times 10^{-2}h_e)k_t \quad (44)$$

$$b_t = (12\epsilon\sigma 273.16^2 + 1.551861h_e)k_t \quad (45)$$

$$c_t = (8\epsilon\sigma 273.16^3 + 44.513596h_e + h_t)k_t \quad (46)$$

$$d_t = (607.919h_e - R_i - h_t T_a - h_e e_a + 2\epsilon\sigma 273.16^4)k_t \quad (47)$$

in which

$$k_t = \frac{1}{2\epsilon\sigma + 5.82436 \times 10^{-4} h_e} \quad (48)$$

$$h_e = \frac{\rho c_p}{\gamma} \frac{g_{sv} g_{bv}}{(g_{sv} + g_{bv})} \quad \text{(for dry leaf)},$$
$$h_e = \frac{\rho c_p}{\gamma} g_{bv} \quad \text{(for wet leaf)} \quad (49)$$

$$h_t = \rho c_p g_{bH} = 0.924 \rho c_p g_{bv} \quad (50)$$

The constants in Eqs. 44 through 48 differ somewhat from those given by Paw U (1987) because we use a different polynomial for computing saturation vapor pressure. Also, in our model, R_i refers to total absorbed radiation from two directions instead from one. Since quartic equations can be solved analytically, leaf temperature can be estimated without iteration for any combination of g_{sv} and g_{bv} (see the appendix).

Next, we eliminate c_i, h_b and c_b from the system. To this end, first we substitute h_b and c_b in Eq. 18 by their equivalents from Eqs. 19 and 20 and rearrange to obtain a quadratic equation for g_{sv}, i.e.

$$a_s g_{sv}^2 + b_s g_{sv} + c_s = 0 \quad (51)$$

where, in case of a dry leaf surface, the coefficients are given by

$$a_s = e_s(T_l) c_b \quad (52)$$

$$b_s = -e_s(T_l)[MA_n - c_b(g_{bv} - b_{sv})] \quad (53)$$

$$c_s = -g_{bv}[MA_n e_a + e_s(T_l) c_b b_{sv}] \quad (54)$$

in which

$$c_b = c_a - A_n \frac{1.37}{g_{bv}} \quad (55)$$

For a wet leaf, Eq. 51 reduces to Eq. 18 with $h_b = 1$. Note that, according to Eq. 51, stomatal conductance is a function of the leaf-boundary layer conductance.

Finally, we substitute C_i in Eqs. 5 and 6 for its equivalent from Eq. 17, then replace W_c and W_j in Eq. 4 by Eqs. 5 and 6, and rearrange to obtain a quartic expression for the net photosynthesis (A_{en}) limited by Rubisco activity and RuBP regeneration capacity, i.e.

$$A_{en}^4 + a_{pn} A_{en}^3 + b_{pn} A_{en}^2 + c_{pn} A_{en} + d_{pn} = 0 \quad (56)$$

$$a_{pn} = [2\alpha r_t^2 R_d - \alpha r_t (2C_a + \varpi) - (V_{cmax} + J/4.5) r_t^2] k_{pn} \quad (57)$$

$$b_{pn} = \{\xi + r_t R_d [r_t(\alpha R_d - V_{cmax} - J/4.5) - 2\alpha(2C_a + \varpi)] + r_t[2C_a(V_{cmax} + J/4.5) + \omega + r_t V_{cmax} J/4.5]\} k_{pn} \quad (58)$$

$$c_{pn} = \{2R_d \xi + r_t R_d [2C_a(V_{cmax} + J/4.5) + \omega - \alpha R_d(2C_a + \varpi)] - C_a[C_a(V_{cmax} + J/4.5) + \omega] + \phi - 2V_{cmax} J r_t (C_a - \Gamma)\} k_{pn} \quad (59)$$

$$d_{pn} = \{R_d[R_d \xi - C_a^2(V_{cmax} + J/4.5) - C_a \omega + \phi] + V_{cmax} J[C_a(C_a - 2\Gamma) + \Gamma^2]/4.5\} k_{pn} \quad (60)$$

in which

$$C_a = c_a P \quad (61)$$

$$k_{pn} = \frac{1}{\alpha r_t^2} \quad (62)$$

$$r_t = P \frac{1.6 g_{bv} + 1.37 g_{sv}}{g_{bv} g_{sv}} \quad (63)$$

$$\phi = \Gamma(2.33 V_{cmax} \Gamma + J K_m / 4.5) \quad (64)$$

$$\xi = \alpha[\Gamma(\Gamma + \varpi) + 2.33 \Gamma K_m] \quad (65)$$

$$\varpi = 2.33\Gamma + K_m \quad (66)$$

$$\omega = 1.33 V_{cmax} \Gamma + J(K_m - \Gamma)/4.5 \quad (67)$$

$$K_m = K_c(1 + O/K_o) \quad (68)$$

Eqs. 51 and 56 are solved analytically and then coded into the algorithm in a way similar to Eq. 43. The net CO_2 assimilation rate (A_n) resulting from all three limitations is estimated by Eq. 1 in which A is calculated from Eq. 3 with $A_e = A_{en} + R_d$.

Thus, we have reduced the original system down to four equations, i.e.

$A_n = \mathbf{f}(g_{sv}, g_{bv}, T_l)$ Eqs. 1, 3, and 56

$g_{sv} = \mathbf{f}(A_n, g_{bv}, T_l)$ Eq. 51

$T_l = \mathbf{f}(g_{sv}, g_{bv})$ Eq. 43

$g_{bv} = \mathbf{f}(T_l)$ Eqs. 29 and 33

A complete list of the model input parameters and output variables is provided in the appendix. An important feature of the new system is that the convergence of all variables is controlled by the stomatal conductance. This allows us to use a simple iterative procedure that only adjusts g_{sv} to obtain a numerical solution (see the appendix for details). The algorithm reaches a global convergence typically within 10 iterations which takes about 0.01 seconds on an IBM-type 386/33MHz personal computer with a math co-processor.

3. Model test

We verified the LEAFC3 model by testing its ability (i) to predict observed leaf CO_2 assimilation rates and stomatal conductances of field-grown plants and (ii) to simulate some well-documented stomatal and photosynthetic responses that have not been explicitly built into its algorithm.

For the photosynthesis test, we used gas-exchange data for lodgepole pine (*Pinus contorta* L.), limber pine (*Pinus flexilis* J.), and quaking aspen (*Populus tremuloides* Michx.). Net photosynthesis rates of lodgepole-pine shoots were measured in 1989 (Schoettle, 1990). Leaf CO_2 assimilation data for limber pine and aspen were provided by Dr. Alan K. Knapp. The lodgepole pine data were collected from the middle and upper portion of the crown of mature trees growing at 2800 m above sea level in southeastern Wyoming (USA). The data for limber pine and aspen originated from tree saplings and lower branches of mature trees at 2600 m above sea level in the same region (Knapp and Smith, 1989). In both studies, a Portable Photosynthesis System (LI-6200, LiCor Inc., Lincoln NE) has been used to measure leaf CO_2 uptake rates, stomatal conductances, and associated environmental variables (i.e. incident PPFD, ambient temperature, relative humidity, and atmospheric CO_2 concentration).

Model predictions of net photosynthesis were compared with 137 instantaneous measurements for lodgepole pine, 94 for limber pine, and 98 for aspen. About one third of the data for each species were used for model parameterization. The biochemical parameters V_{m25}, J_{m25}, K_{c25}, K_{o25}, and f were estimated applying a method similar to one proposed by Ziegler-Jöns and Selinger (1987). The m and b_{sv} parameters were calculated by a linear regression from measured data on stomatal conductance, net photosynthesis, relative humidity, and atmospheric CO_2 concentration. Since none of the data sets contained information on xylem leaf water potential, it was uniformly assumed that leaf water deficit reduced stomatal conductance by 1%. Table 1 lists the

Table 1
Species-specific input parameter values used by the LEAFC3 model (see text for parameter explanation)

Parameter	*Pinus contorta*	*Pinus flexilis*	*Populus tremuloides*	Units
V_{m25}	43.31	99.85	53.00	μmol m^{-2} s^{-1}
J_{m25}	100.05	175.34	64.66	μmol m^{-2} s^{-1}
K_{c25}	27×10^{-5}	27×10^{-5}	45×10^{-5}	mol/mol
K_{o25}	41×10^{-2}	41×10^{-2}	30×10^{-2}	mol/mol
f	0.48	0.45	0.64	–
m	9.75	8.70	13.50	–
b_{sv}	7.52	18.40	73.30	mmol m^{-2} s^{-1}
d	1×10^{-3}	1×10^{-3}	41×10^{-3}	m
d_o	75×10^{-3}	60×10^{-3}	41×10^{-3}	m

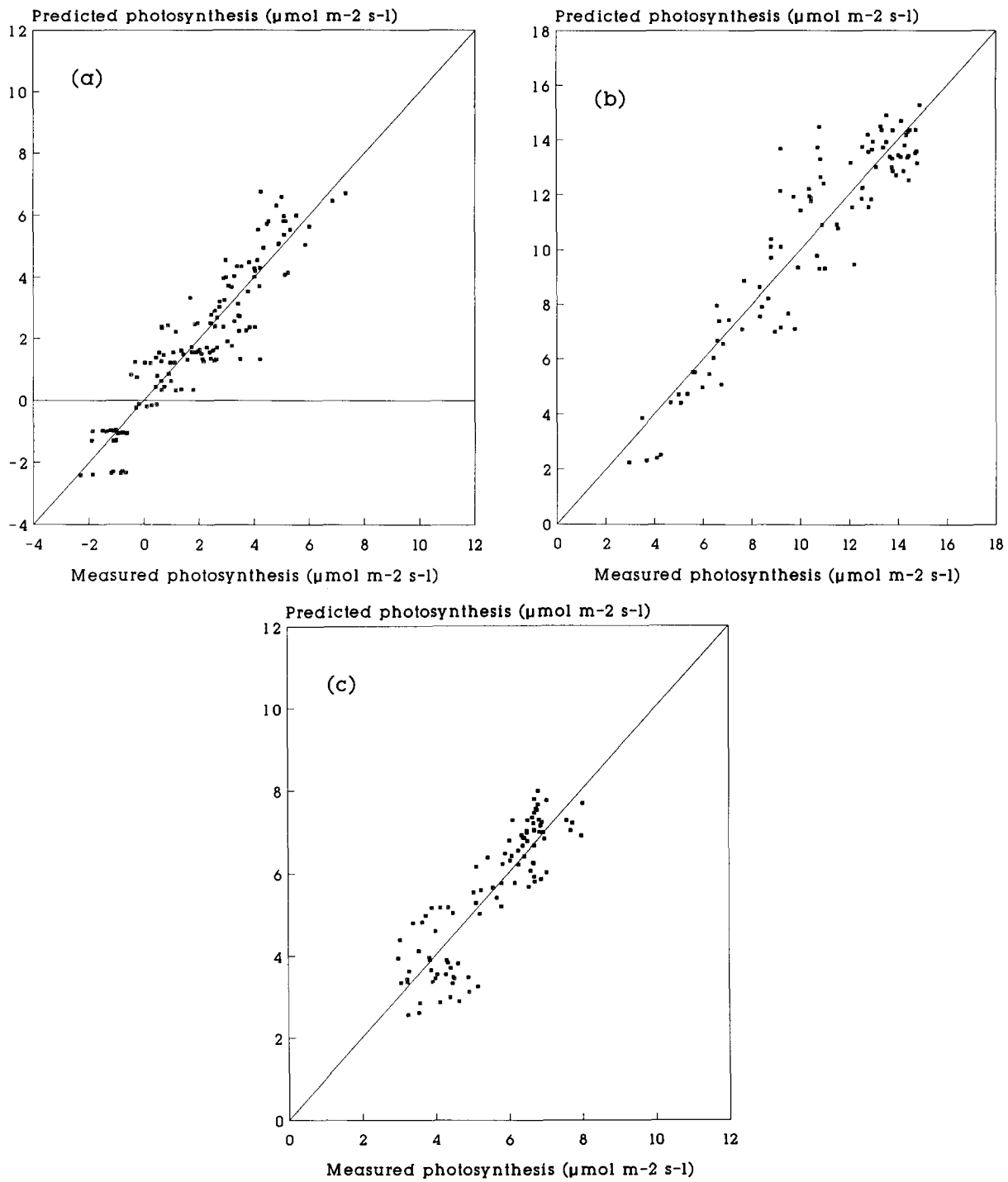

Fig. 1. Comparison of measured rates of net photosynthesis with rates predicted by the LEAFC3 model using parameter values in Table 1. Mode performance is evaluated by the Pearson's correlation coefficient (r), the slope of the regression line between observed and predicted rates (s), and the line intercept (I). (a) Lodgepole pine, $r = 0.92$, $s = 1.00$, $I = 0.00$. (b) Limber pine, $r = 0.93$, $s = 1.00$, $I = 0.00$. (c) Quaking aspen, $r = 0.87$, $s = 1.00$, $I = 0.01$.

parameter values estimated for the studied species. Although the LI-6200 instrument also measured leaf stomatal conductances, in both studies, there were not enough independent data to test model predictions of stomatal response. In the case of lodgepole pine, most measurements were taken on partially wet branches which significantly obscured reported conductance values. On the other hand, stomatal conductances for limber pine and aspen provided by Knapp were reliable but in most cases in disequilibrium with net photosynthesis. The few suitable stomatal conductance data for each species were used to estimating the parameters m and b_{sv} in Eq. 18. Due to a linear relationship in the model between leaf conductance and photosynthesis, one can expect that testing predictions of net CO_2 uptake rates provides a sound basis for assessment of model credibility. Nevertheless, we used stomatal conductance data collected by Kaufmann (1982a,b) in 1980 to perform an independent model test. Kaufmann (1982a,b) used an automatic cuvette system (Kaufmann, 1981) to record hourly changes of leaf physiological conductance to water vapor in four subalpine tree species growing at 2900 m above sea level at the Fraser Experiment Forest near Fraser, Colorado USA. The system also measured air temperature, atmospheric humidity, and incident PPFD on a horizontal surface. We ran the LEAFC3 model using the parameter values for lodgepole pine in Table 1, and the environmental data provided by the cuvette system to predict 237 instantaneous stomatal responses from July 13 through August 26. Model estimates were then compared with conductance measurements for lodgepole pine.

Fig. 1a presents a plot of simulated versus actual net CO_2 assimilation rates for lodgepole pine. The correlation (r) between measured and predicted photosynthesis is 0.92 with a regression slope (s) of one and an intercept (I) not significantly different from zero. The scatter around the

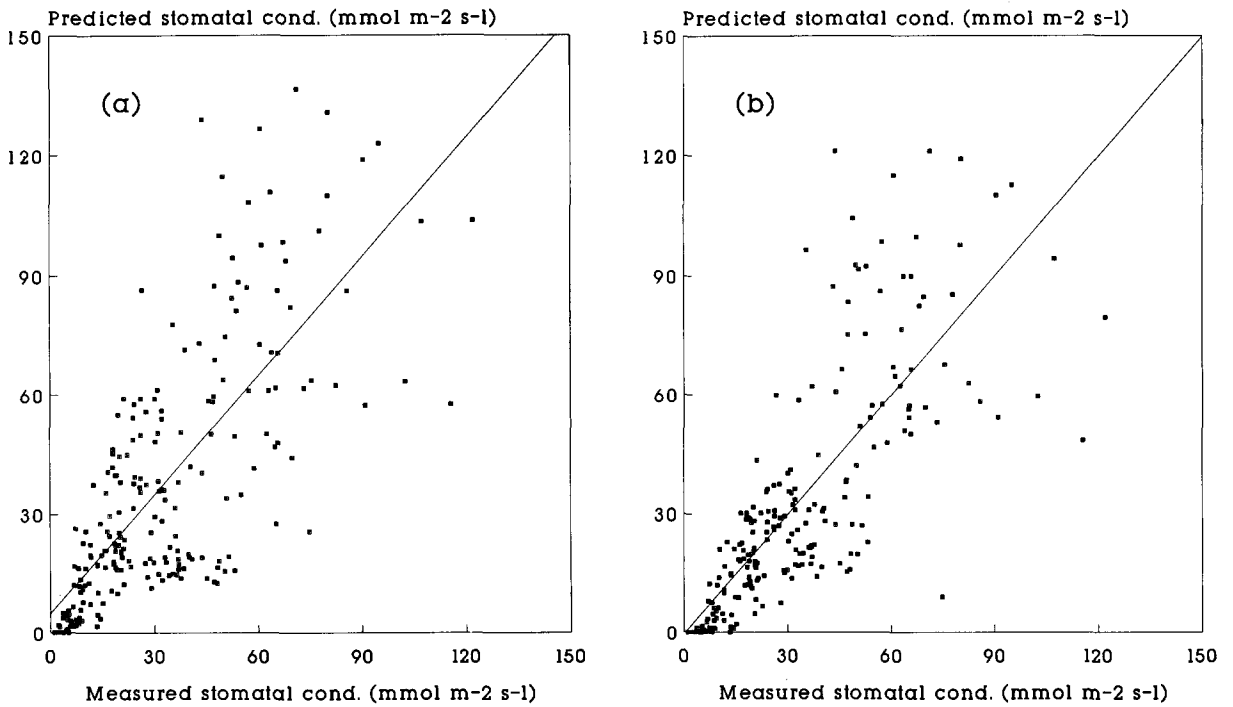

Fig. 2. Comparison between measured and predicted stomatal conductances for lodgepole pine. Experimental data are from Kaufmann (1982a,1982b). (a) No reduction imposed on reported PPFD data, $r = 0.75$, $s = 1.00$, $I = 4.87$; (b) PPFD data reduced by 49%, $r = 0.80$, $s = 1.00$, $I = -0.30$.

straight line is caused, in part, by differences in the light-use efficiency of needles from various levels in the canopy. For example, when model estimates are only compared with data obtained from the upper portion of tree crown, Pearson's r increases to 0.95 (not shown). The correspondence between measured and predicted photosynthetic rates for limber pine was $r = 0.93$ (Fig. 1b). The lower correlation coefficient for aspen, $r = 0.87$ (Fig. 1c) is, perhaps, due to a greater variability in the photosynthetic capacity among the leaves of this species. Overall, the model explained most of the variation in the CO_2 assimilation data for the studied species. Fig. 2 presents the correspondence between measured and predicted stomatal conductances of lodgepole pine for the Kaufmann's data set. Despite a somewhat lower correlation coefficient compared to one for photosynthesis, the model accounts for about 64% (Fig. 2b) of the variation in observed data. Yet a significant portion of the variation remains unexplained. Kaufmann (1982a) also pointed out the large variability in the measured data. It is unknown, however, how much of this variability is real, and how much is attributable to the measuring system. For example, we found that model predictions improve (as indicated by the r and I values in Figs. 2a and 2b) when reported PPFD data are reduced by 49%. Our hypothesis is that shoot structure and orientation create a shading pattern that substantially reduces the amount of PPFD incident on a unit of needle surface area compared to that received on a horizontal plane. The LEAFC3 model is sensitive to changes in incident short-wave radiation as they affect both leaf energy balance and photochemical reactions. The reduction coefficient for PPFD, which we found empirically, is in good agreement with similar estimates obtained for scotch pine shoots by Smolander et al. (1987).

To further verify the underlaying model concept, we performed a sensitivity test in which the

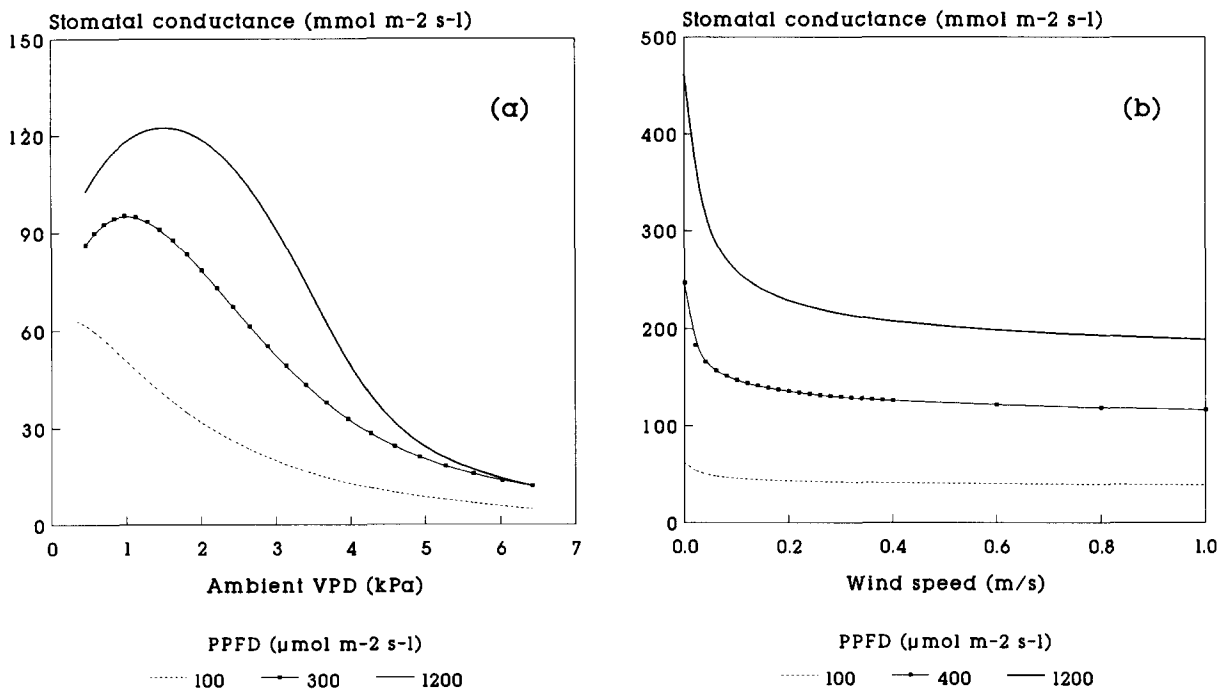

Fig. 3. Predicted responses of stomatal conductance to: (a) changes in ambient water-vapor pressure deficit (VPD) for lodgepole pine ($g_{bv} = 3.2$ mol m^{-2} s^{-1}); and (b) variations in wind speed for limber pine ($T_a = 25°$ C, ambient relative humidity = 40%). Changes in VPD are simulated by varying air temperature at a constant vapor pressure.

model was applied to simulate several observed leaf-environmental relationships that have not been explicitly coded into its structure. The test was done using the species parameter values in Table 1. Unless stated otherwise, all simulations assume an ambient O_2 concentrations of 209 mmol/mol and a well ventilated leaf surface.

Fig. 3a portrays the predicted apparent response of stomatal conductance of lodgepole pine to changes in ambient water-vapor pressure deficit (VPD) at three irradiance levels. The change in VPD is simulated by using a constant vapor pressure of 1.36 kPa and increasing air temperature from 15° C to 41° C. The relationship produced by the model is typical for tree species (Waring and Schlesinger, 1985).

Grace et al. (1975), Dixon and Grace (1984) and others found experimentally that leaf stomatal conductance increases exponentially with decreasing wind speed. This effect was recently confirmed in a semi-experimental study by Aphalo and Jarvis (1993b) as well. Fig. 3b illustrates that the LEAFC3 model successfully simulates the observed pattern of wind-induced changes in stomatal conductance. Such a response is due to feedbacks operating between stomatal conductance and the humidity and CO_2 concentration levels at the leaf surface. The latter are partially controlled by the leaf-boundary layer conductance which is a function of leaf size and wind speed (see Eqs. 29 and 51).

Another observed phenomenon is the effect of radiation intensity on the temperature response of net CO_2 assimilation and stomatal conductance. The model correctly predicts a shift of the photosynthetic optimum toward higher temperatures with increasing irradiance (Fig. 4a) (Berry and Björkmann, 1980). Osonubi and Davies (1980) observed that, under constant VPD and low irradiance, leaf stomates respond to temperature with a broad-topped optimum, and the temperature sensitivity of stomatal conductance increases with PPFD. Fig. 4b presents the relationship between g_{sv} and temperature predicted by the model for

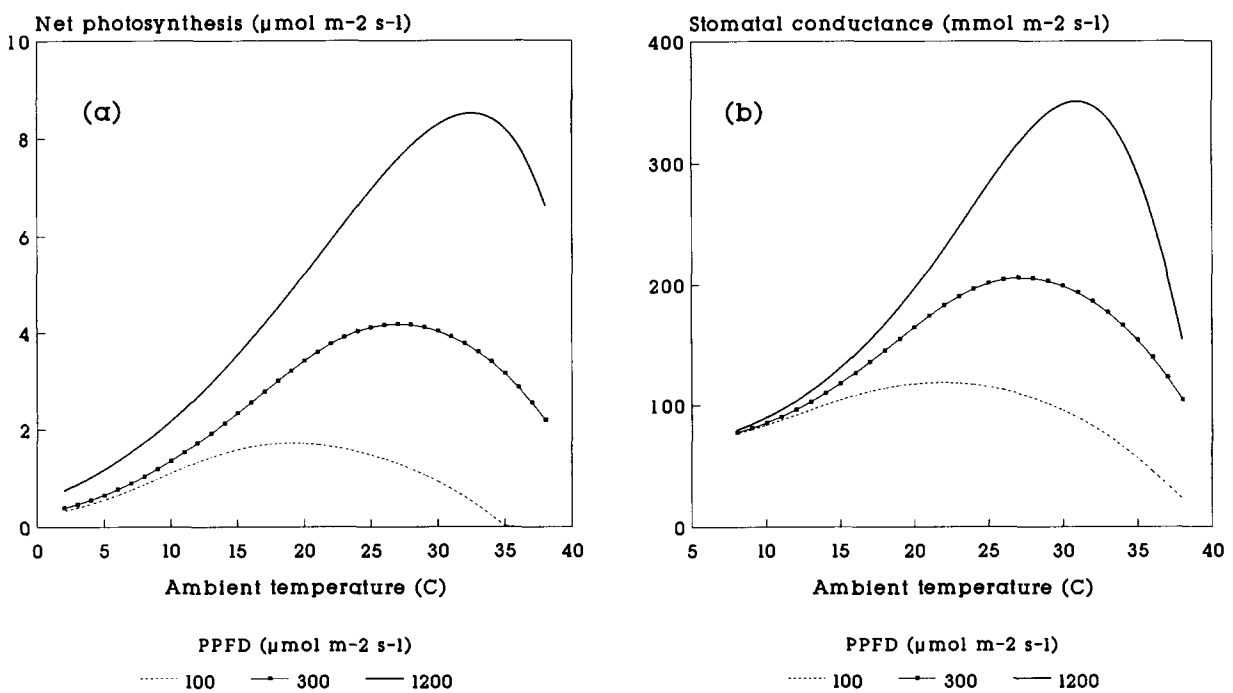

Fig. 4. Modeled effect of incident photosynthetic photon flux density on the temperature response of (a) net photosynthesis at 40% relative humidity, and (b) stomatal conductance at VPD = 1.0 kPa in aspen (g_{bv} = 1.8 mol m^{-2} s^{-1}).

an aspen leaf under VPD of 1 kPa and three irradiance levels. It follows the pattern described by Osonubi and Davies (1980).

Water-use efficiency (WUE), i.e. the amount of net CO_2 uptake per unit of water transpired, is an index that combines the effect of leaf biochemical and stomatal responses. WUE has been found to decline exponentially with increasing atmospheric VPD both in agricultural crops and in forest trees (Sinclair et al., 1984; Zur and Jones, 1984; Baldocchi et al., 1987). This relationship is predicted by the LEAFC3 model. Fig. 5 displays the simulated response of WUE to ambient VPD in limber pine. Changes in VPD are simulated by keeping vapor pressure constant and varying air temperature.

In a paper that argues against the Ball–Berry stomatal model (Eq. 18), Aphalo and Jarvis (1991) present, as one of their strongest arguments, experimental data showing that, under low irradiance and constant VPD, the stomates of *Hedera helix* remain unresponsive or close with increasing leaf-surface relative humidity, an observation which seems to be contradicting the stomatal model. However, the LEAFC3 model was able to simulate such an effect. Fig. 6 portrays the predicted stomatal response of limber pine to leaf-surface relative humidity at PPFD = 120 μmol m^{-2} s^{-1}, and VPD = 1.0 kPa. The change in humidity is achieved by varying the ambient temperature from 17° C to 37° C. The explanation for this reversed stomatal response, in the model context, is that, at low PPFD, gross photosynthesis is constrained by the rate of RuBP regeneration which becomes, under such conditions, almost insensitive to temperature. Thus, increasing leaf temperature enhances dark- and photo-respiration without significantly promoting carboxylation. As a result, net CO_2 assimilation decreases faster than leaf-surface humidity increases which

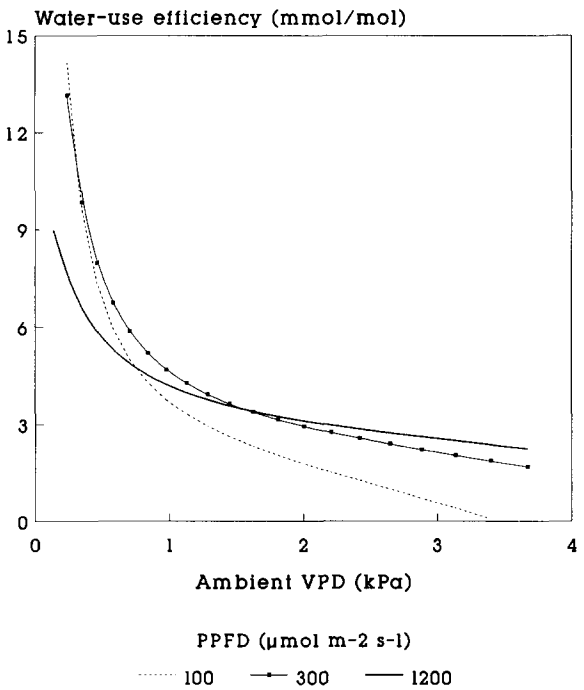

Fig. 5. Relationship between leaf water-use efficiency (mmol CO_2 /mol H_2O) and atmospheric vapor pressure deficit predicted by the model for limber pine. Changes in VPD are simulated by varying air temperature at a constant vapor pressure.

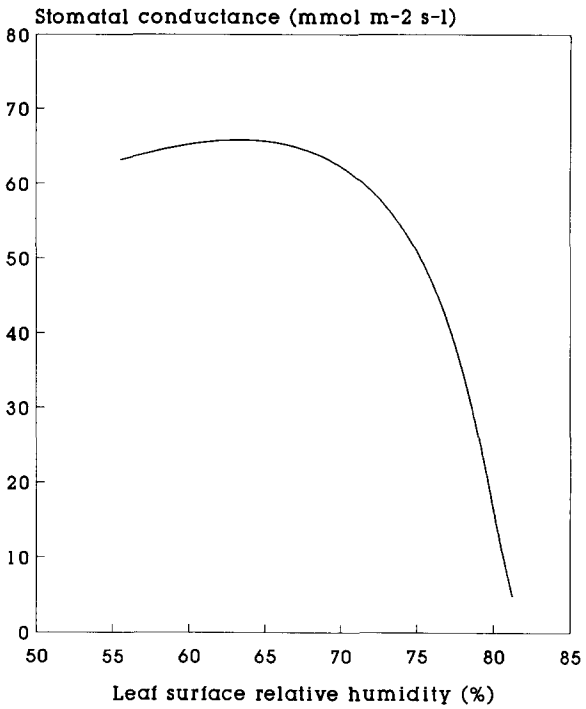

Fig. 6. Predicted response of the stomatal conductance of limber pine to variations in leaf-surface relative humidity at VPD = 1.0 kPa and PPFD = 120 μmol m^{-2} s^{-1}.

produces, eventually, a decline in stomatal conductance.

Figs. 7a and 7b show model predictions of net photosynthesis and stomatal conductance to an increasing atmospheric CO_2 concentration. An almost linear enhancement of CO_2 assimilation accompanied by a decline of stomatal aperture have been observed in many studies investigating the short-term effect of CO_2 increase (Oechel and Strain, 1985; Eamus and Jarvis, 1989). While net assimilation has always been found to increase in CO_2-enriched environments, reports on changes of stomatal conductance have been controversial ranging from a significant decline to a slight increase (Eamus and Jarvis, 1989). Our model projects that stomatal response to changes in atmospheric CO_2 depends not only on leaf physiological properties but also upon imposition of other environmental stresses such as low humidity or drought, with stomates becoming less sensitive to ambient CO_2 when under higher stress (Fig. 7b). This prediction is supported by experimental evidence. For example, Beadle et al. (1979) found that CO_2-induced stomatal closure in Sitka spruce (*Picea sitchensis* Carr.) is greatly diminished by water stress.

Several studies with C_3 and C_4 plants have reported that photosynthetic enhancement by elevated CO_2 concentration increases almost linearly with temperature over the range 10° C–35° C (e.g. Lemon, 1983; Idso et al., 1987; Rawson, 1992). This phenomenon is predicted by the LEAFC3 model. Fig. 8a presents the simulated increase of net CO_2 assimilation in limber pine caused by a doubled atmospheric CO_2 concentration (i.e. 680 μmol/mol) as a function of air temperature and incident PPFD. The shape of the projected relationship closely resembles the pattern observed by Idso et al. (1987). The model also predicts that the relative photosynthetic response to elevated CO_2 concentration increases with decreasing atmospheric humidity (or falling

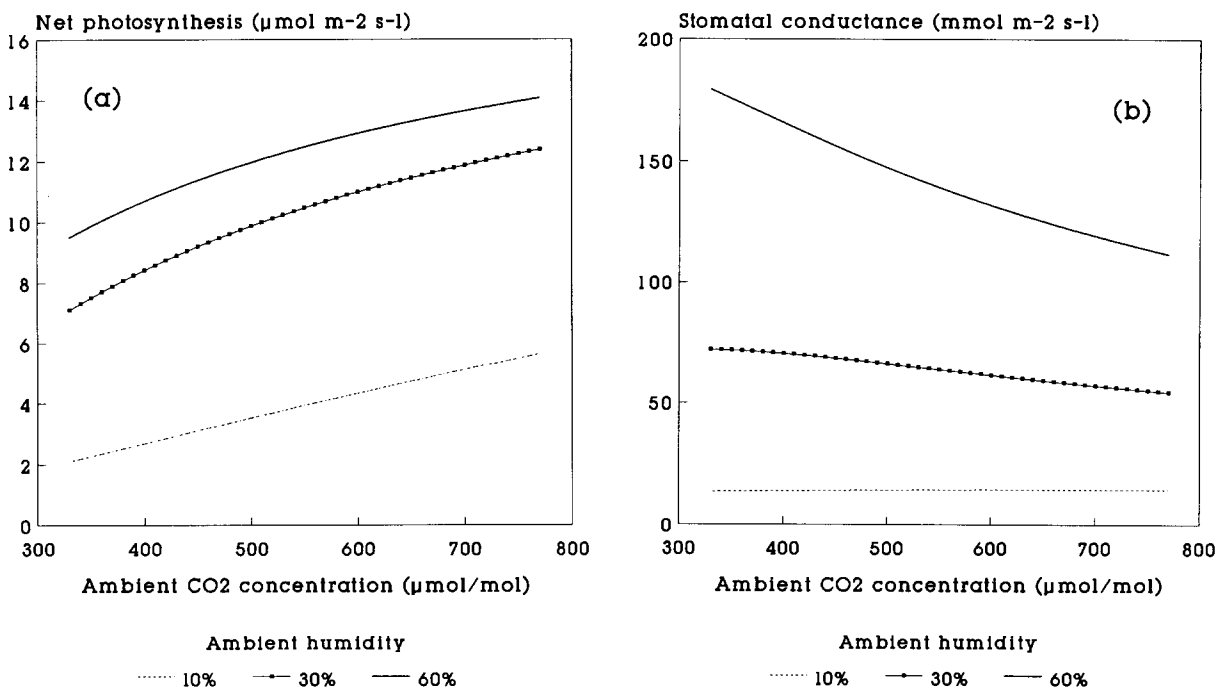

Fig. 7. Modeled effect of changes in atmospheric CO_2 concentration on net photosynthesis (a), and stomatal conductance (b) in lodgepole pine at $T_a = 25°$ C, PPFD = 1000 μmol m^{-2} s^{-1}, and $g_{bv} = 2.9$ mol m^{-2} s^{-1}.

xylem water potential) (Fig. 8b), an effect which has been registered experimentally as well (Kimball, 1985; Eamus and Jarvis, 1989).

4. Environmental and physiological regulation of leaf water-use efficiency under steady-state conditions

WUE is a key functional characteristic of the vegetation. At the scale of an individual, it constrains plant's potential for growth and survival in areas with limited water supply. At the landscape level, it determines the linkage between watershed hydrology and ecosystem net primary productivity. Since the functioning of plant canopies strongly depends on leaf responses (Baldocchi, 1993; Norman, 1993), knowing the factors that control changes of WUE at the leaf level is of both scientific and practical importance.

We applied the LEAFC3 model to study the impact of leaf physiological properties and environmental factors on the water-use efficiency of lodgepole pine and aspen under equilibrium conditions. These species were selected for different stomatal and photosynthetic sensitivities to environmental perturbations based on the parameter values in Table 1. Responses of leaf WUE were investigated to variations of wind speed, solar radiation, air temperature, vapor pressure deficit, ambient CO_2 concentration, and atmospheric pressure.

4.1. Incident radiation

Figs. 9 and 10 present species responses of leaf WUE to changes in PPFD under three wind velocities and two humidity levels. At wind speeds greater than 0.1 m/s, WUE peaks at PPFD of ca. 320 μmol m^{-2} s^{-1} in both species. A poor leaf

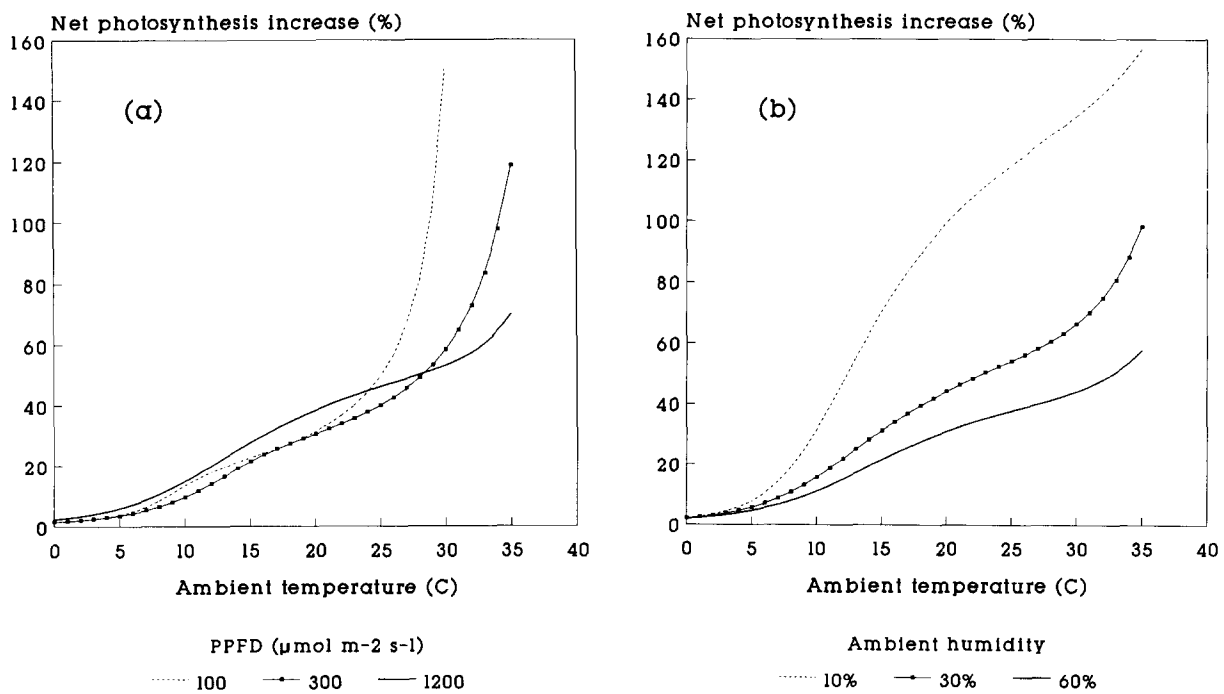

Fig. 8. Modeled effect of air temperature on net photosynthetic increase in limber pine caused by doubled atmospheric CO_2 concentration (a) at 40% relative humidity and three radiation levels, and (b) at PPFD = 1000 μmol m^{-2} s^{-1} and three humidity levels.

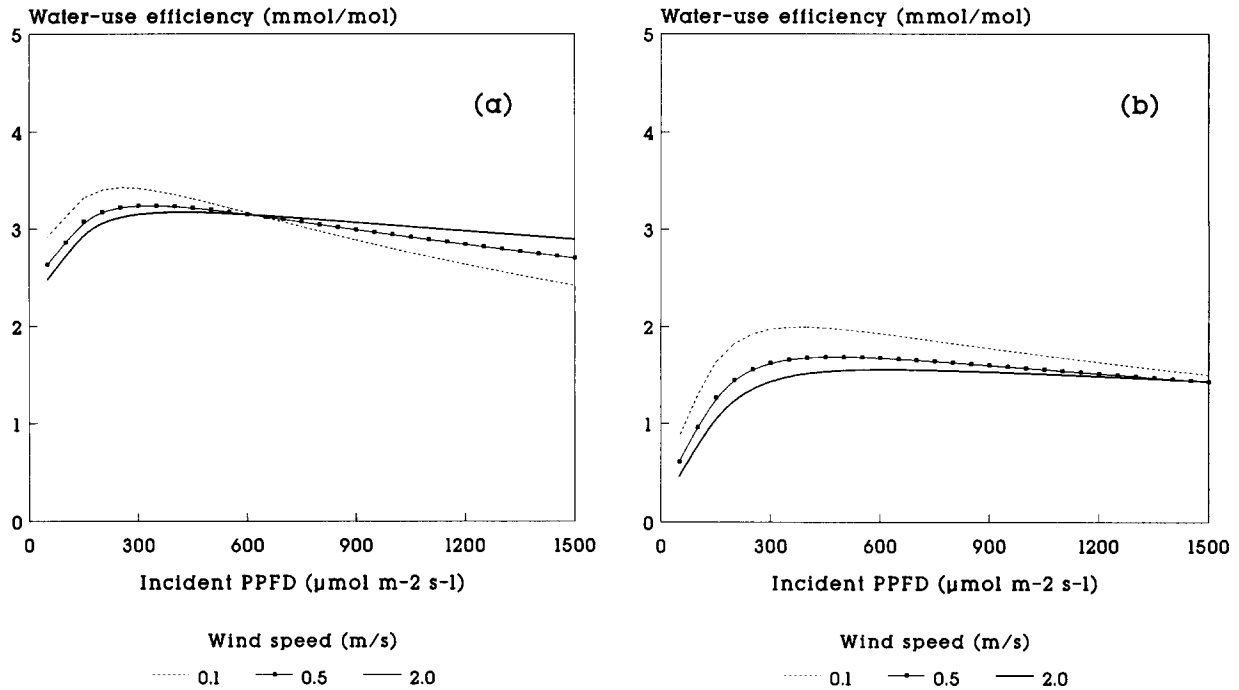

Fig. 9. Modelled response of leaf water-use efficiency to variations of incident PPFD and wind velocity at $T_a = 25°$ C and 40% relative humidity in (a) lodgepole pine, and (b) aspen.

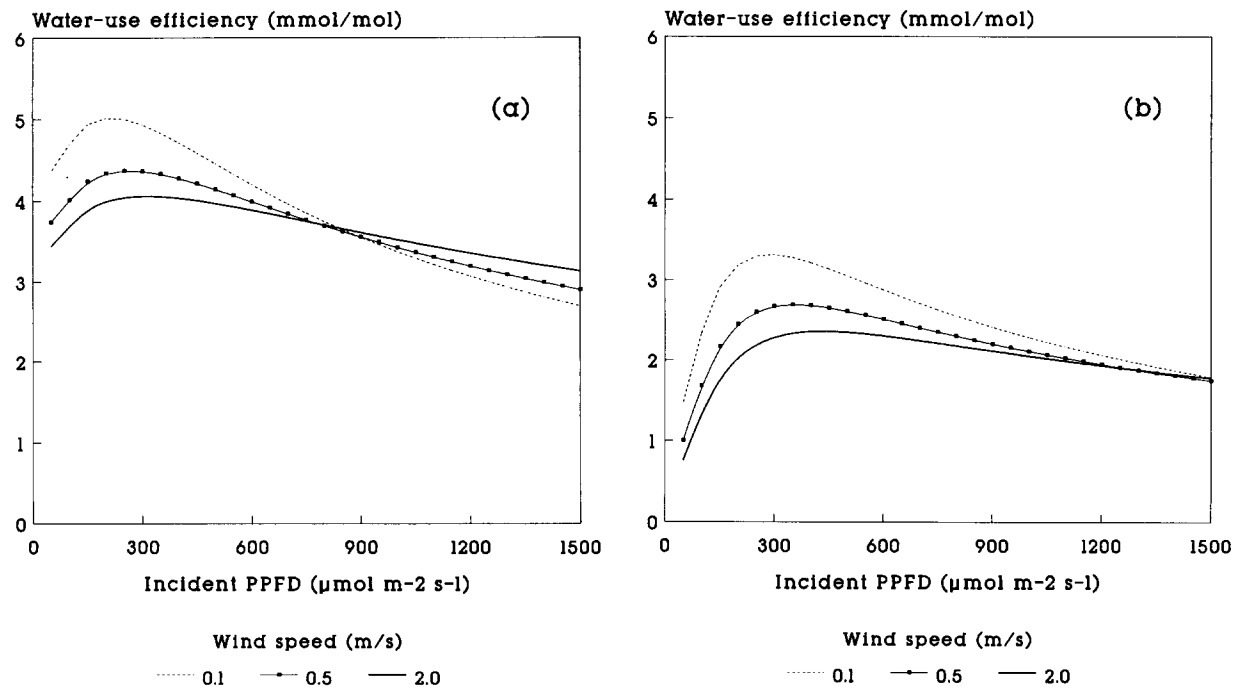

Fig. 10. The same response as in Fig. 9 but at 70% relative humidity.

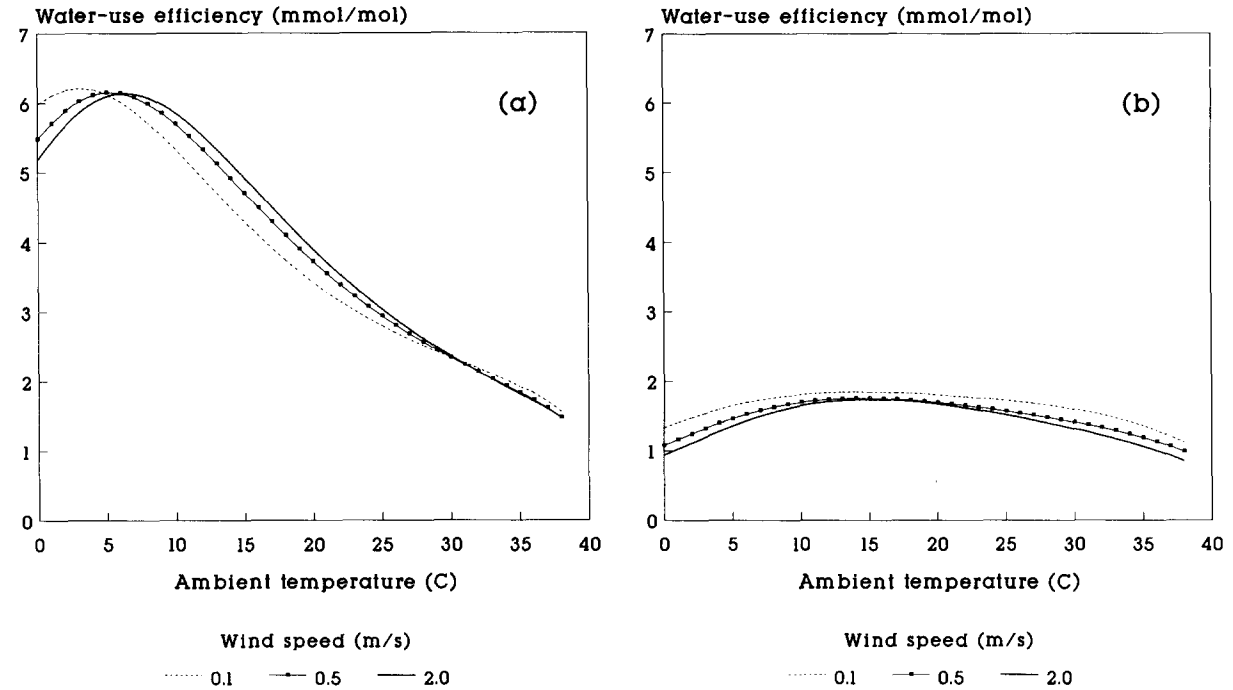

Fig. 11. Predicted response of leaf water-use efficiency to variations of ambient temperature and wind velocity at 40% relative humidity and PPFD = 1000 μmol m^{-2} s^{-1} in (a) lodgepole pine, and (b) aspen.

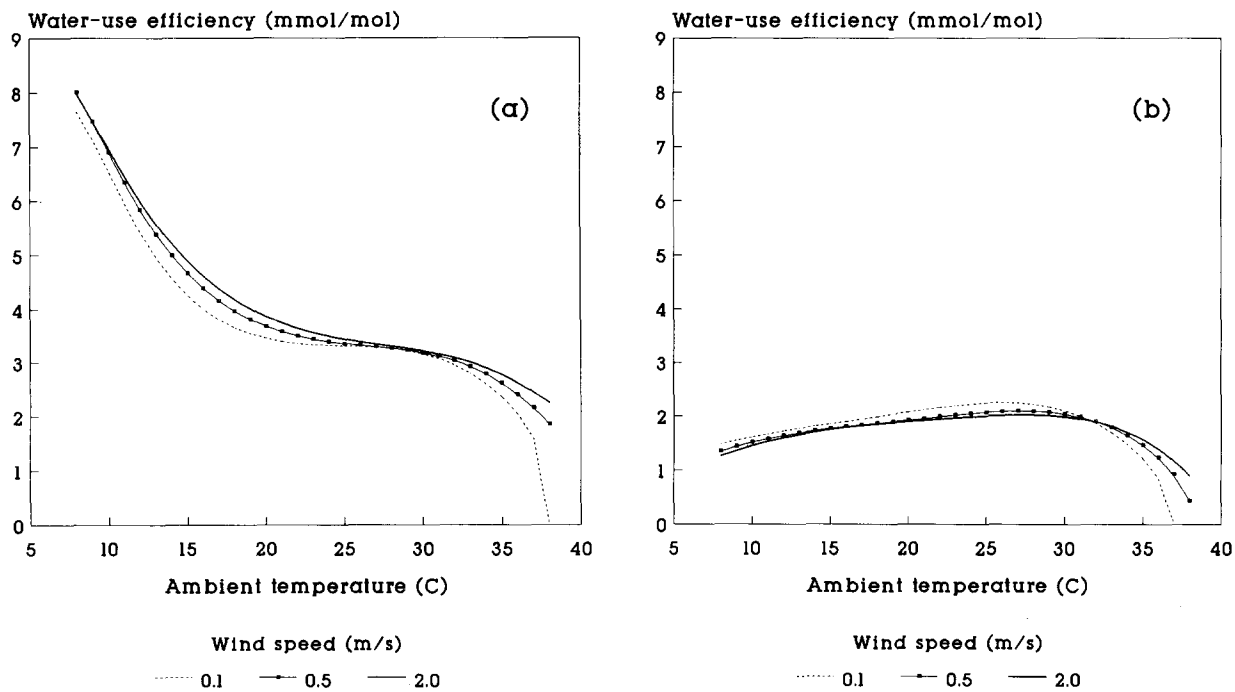

Fig. 12. The same response as in Fig. 11 but under constant VPD of 1 kPa.

ventilation shifts the WUE maximum toward lower PPFD. WUE declines steadily as PPFD increases above 320 because high radiation levels enhance transpiration more than they do photosynthesis through rising leaf temperature and steepening leaf-to-air vapor pressure gradient. Lower PPFD, on the other hand, cause a drop of WUE due to a declining CO_2 assimilation rate. Low wind speeds diminish the control of leaf stomata over transpiration by reducing leaf-boundary layer conductance and increasing leaf surface humidity. This amplifies the radiation effect on WUE. The radiative sensitivity of WUE also increases with ambient humidity (Fig. 10). This occurs because, at intermediate irradiance, high atmospheric humidity enhances net CO_2 uptake by increasing stomatal conductance and decreases transpiration by reducing leaf-to-air water-vapor concentration gradient. Lodgepole pine is predicted to have a WUE about twice as high as that of aspen. These diverse species responses follow mainly from different values for the parameters m, b_{sv}, and J_{m25}. The large m and b_{sv} values in aspen produce high stomatal conductance that feeds back to photosynthesis yielding a relatively low WUE.

4.2. Air temperature

The model predicts qualitatively different temperature responses of WUE for the studied species (Fig. 11). While aspen maintains a nearly constant WUE over the temperature range 5° C–35° C, the WUE of lodgepole pine continuously declines from about 6 to 1.5 mmol/mol. In both species, the WUE response under constant relative humidity is similar to that under constant VPD (Figs. 11 and 12). This indicates that the temperature sensitivity of leaf WUE is predominantly controlled by intrinsic physiological factors. Our analysis showed that the most important mechanisms in this regard are the ones that regulate the ratio of stomatal conductance to net photosynthesis.

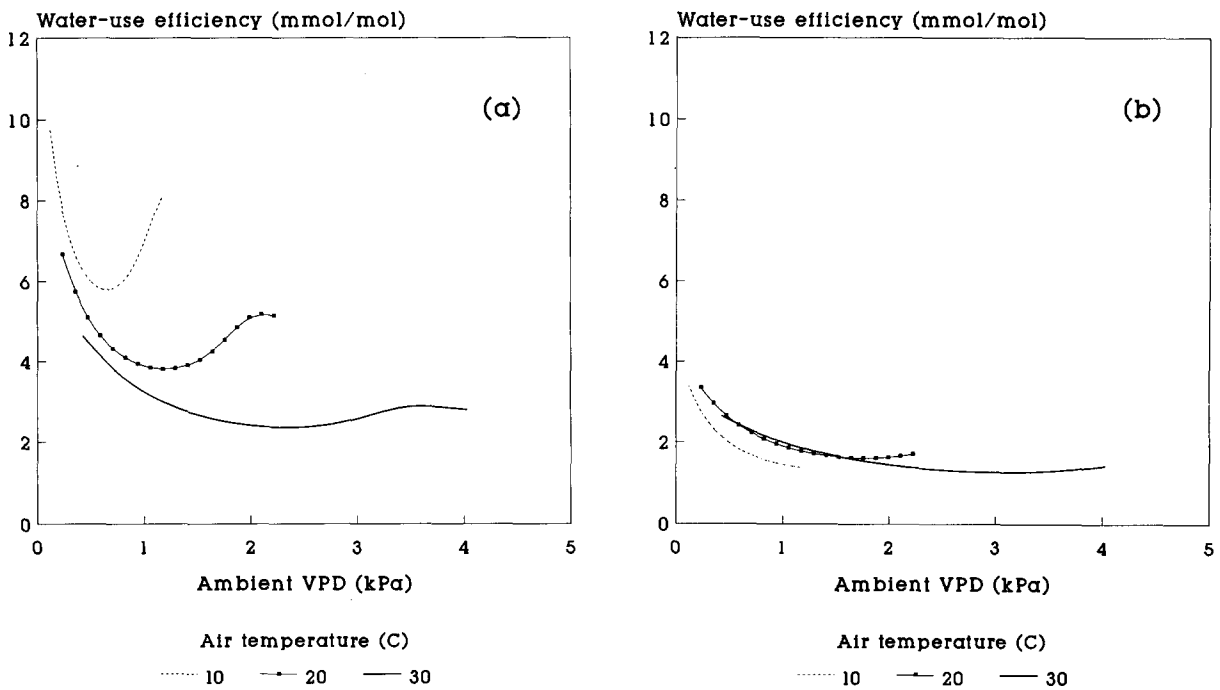

Fig. 13. Modeled response of leaf water-use efficiency to variations of ambient vapor pressure deficit and air temperature at a wind speed of 2 m/s, and PPFD = 1000 μmol m^{-2} s^{-1} in (a) lodgepole pine, and (b) aspen. Changes in VPD are simulated by altering relative humidity under constant temperature.

4.3. Vapor pressure deficit

The form of the functional relationship between atmospheric VPD and leaf WUE depends on what generates changes in VPD. Leaf WUE declines exponentially with VPD when the latter increases as a result of rising air temperature under constant vapor pressure. In this case, lodgepole pine and aspen show WUE responses that are similar in shape to one portrayed in Fig. 5. However, pine is predicted to have a much higher WUE sensitivity than aspen. Since in non-desert areas, diurnal changes of VPD are mostly caused by temperature variations, the negative exponential relationship has been typically observed in field experiments (Tanner and Sinclair, 1983; Sinclair et al., 1984; Zur and Jones, 1984; Baldocchi et al., 1987). However, changes in VPD can be also induced by seasonal and/or spatial variations of water vapor content in the air. Leaf WUE exhibits a qualitatively different response to VPD when the latter varies as a result of changing relative humidity at a constant temperature. Under such conditions, WUE decreases to a minimum and then increases again (Fig. 13). The vapor pressure deficit at which the minimum in WUE occurs depends on temperature, and is higher at warmer temperatures. In lodgepole pine, ambient temperature also significantly affects the magnitude of the WUE minimum. In aspen, this effect is considerably weaker due to a lower temperature sensitivity of WUE in this species (Figs. 11b and 12b). Again, the divergence in species responses was found to be mainly a result of build-in physiological disparities related to the model parameters V_{m25}, J_{m25}, m, and b_{sv}.

4.4. Ambient CO_2 level

As a result of opposite responses of net photosynthesis and stomatal conductance to changes in CO_2 concentration (see Fig. 7), leaf WUE increases linearly as atmospheric CO_2 enhances from 300 μmol/mol to 800 μmol/mol. The projected rates are 31% per 100 μmol CO_2 for lodgepole pine and 21% for aspen. Poor leaf ventilation and low atmospheric humidity cut back these rates by about 5%.

4.5. Atmospheric pressure

Reduction of barometric pressure increases leaf-boundary layer conductance (Eqs. 29 and 33) which enhances transpiration. Pressure changes, however, do not affect net photosynthesis since the ratio of carboxylation to photorespiration (Γ/C_i) is independent of pressure. As a result, leaf WUE drops linearly when pressure falls down. The predicted decline is between 7.7% and 14.2% per 10 kPa and depends weakly on species and wind velocity. This does not necessary imply that plants from high altitudes would have lower WUE compared to individuals of the same species growing at low elevations. The effect of atmospheric pressure on WUE is mild and can be easily offset by altitudinal changes in ambient temperature and humidity. This is particularly true for species whose WUE is positively influenced by low temperatures such as lodgepole pine (Figs. 11 and 12).

The results from the above simulation experiment can be summarized as follows:

a. Leaf water-use efficiency varies not only with atmospheric vapor content and CO_2 concentration as suggested by Sinclair et al. (1984) but with temperature, radiation and atmospheric pressure as well.
b. Wind velocity can sizably modify the effect of physical factors on WUE especially under moderate irradiances.
c. Leaf physiology plays a strong regulatory role in the WUE responses which suggests that there might be significant differences in the magnitude and environmental sensitivity of WUE among plant species.

5. Conclusion

We presented a generic model for estimating short-term fluxes of carbon dioxide, water vapor, and heat from broad leaves and needle-leaved coniferous shoots of C_3 plants. The model combines, in a mathematically consistent and compu-

tationally efficient form, all major processes and feedbacks known to have an impact on the leaf biophysics and biochemistry. An explicit simulation of leaf-boundary layer mechanisms allows the model to account for effects of air flow, leaf geometry, and atmospheric pressure on the leaf energy and gas exchange, as well as for feedbacks taking place under low wind speeds between boundary-layer conductance and leaf stomatal conductance. Test results have demonstrated that the model is capable of predicting complex leaf-environmental interactions such as mutual effects of CO_2, temperature, irradiance, humidity, and wind speed on net photosynthesis, stomatal conductance, and transpiration.

The model assumes a linear relationship between net CO_2 assimilation and stomatal conductance (Eq. 18) and does not account for changes in the heat storage of leaves (Eq. 37). This restricts its application to steady-state conditions, i.e. LEAFC3 does not simulate transient leaf responses to environmental fluctuations that occur over periods of seconds to a few minutes. For example, radiation intensity can experience sizable variations over such time intervals due to either intermittent cloud cover or wind-induced changes of the shading pattern inside plant canopies (Knapp and Smith, 1989). Abrupt changes in PPFD produce temporary decoupling of stomatal conductance from net photosynthesis followed by an exponential recovery pattern in g_{sv} (Knapp and Smith, 1989,1990; Knapp, 1993). This occurs because leaf biochemical machinery responds much faster to variations in sunlight compared to stomatal kinetics. The time required by the leaf system to return to equilibrium under the new conditions seems to depend upon growth form and the type of photosynthetic pathway. Experimental data obtained by Knapp and Smith (1989) and Knapp (1993) suggest that this time is in the order of 15–19 min for C_3 and woody vegetation, and of 5–13 min for C_4 and herbaceous plant species. Hence, the LEAFC3 model should be used with micro-meteorological data that represent at least 20-min averages. This makes the model suitable for incorporation into many fine-resolution ecosystem models with an hourly time step of computation. However, an important question to be answered by the future research is, how successfully a steady-state model can predict average leaf photosynthetic and transpiration rates over time periods where the physical environment has been subjected to random and frequent perturbations. We hope that our model will help address this question as well.

Acknowledgements

The development of the LEAFC3 model is sponsored by the USDA FS Interior West Global Change Program and the Terrestrial Ecosystem Regional Research and Analysis (TERRA) Laboratory in Fort Collins CO USA. The authors thank Dr. Alan K. Knapp for providing the LI-6200 LiCor gas-exchange data, Dr. Merrill Kaufmann for providing stomatal conductance data, Dr. Douglas G. Fox (Director of the TERRA Laboratory) for his support and comments on an early draft of this paper, Drs. Michael G. Ryan, Rudy M. King, and Karl F. Zeller from the USDA FS Rocky Mountain Forest and Range Experiment Station, and Drs. Michael B. Coughenour and Dean Urban from the Colorado State University as well as two anonymous reviewers for valuable suggestions.

Appendix 1

Listed below is the computer code of the LEAFC3 model. It is written as a Turbo-Pascal unit (version 4.0 and higher) that can be easily incorporated into plant canopy models. Procedure *LeafC3* is the main program of the model. It uses functions *LBLCond, LeafTemp, StomCond,* and *C3NetAssim*. The input and output parameters and their units required by the procedure *LeafC3* are as follows (the corresponding symbols used in text are shown in parentheses):

Input parameters

Species-specific parameters:

Vm25	Maximum carboxylation velocity at 25° C,	μmol m^{-2} s^{-1}	(V_{m25})
Jm25	Light-saturated potential rate of electron transport at 25° C,	μmol m^{-2} s^{-1}	(J_{m25})
Kc25	Kinetic parameter for CO_2 at 25° C	mol/mol	(K_{c25})
Ko25	Kinetic parameter for O_2 at 25° C,	mol/mol	(K_{o25})
f	PPFD loss factor,	-	(f)
m	Composite stomatal sensitivity,	-	(m)
Bs	Empirical constant for stomatal conductance,	mol m^{-2} s^{-1}	(b_{sv})
Dleaf	Leaf width (or needle diameter),	m	(d)
Dshoot	Shoot diameter (for conifers only),	m	(d_o)
Pcr	Critical leaf water potential,	(negative MPa)	(Ψ_{crit})
Npw	Power term used in the relationship between stomatal conductance and leaf water potential,	-	(n)

Environmental parameters:

Plw	Leaf xylem water potential,	(negative MPa)	(Ψ)
Pa	Atmospheric pressure,	Pa	(P)
Ca	Ambient CO_2 concentration,	mol/mol	(c_a)
Oa	Ambient oxygen concentration,	mol/mol◦	(-)
Ta	Ambient air temperature,	C	(T_a)
RH	Ambient relative humidity,	%	(-)
Ri	Bi-directional absorbed short- and long-wave radiation by the leaf,	W/m^2	(R_i)
PPFD	Incident photosynthetic photon flux density,	μmol m^{-2} s^{-1}	(Q)
WSpeed	Wind velocity,	m/s	(u)
Wstat	Leaf wetness status,	0 – dry, 1 – wet	(-)

Output variables

An	Net CO_2 assimilation rate,	μmol m^{-2} s^{-1}	(A_n)
Gs	Stomatal conductance to water vapor,	μmol m^{-2} s^{-1}	(g_{sv})
Gb	All-sided leaf-boundary layer conductance to water vapor,	μmol m^{-2} s^{-1}	(g_{bv})
Tl	Leaf temperature,	°C	(T_l)
LHeat	Latent heat flux,	W/m^2	(-)

The interface section of the unit assigns default values to a number of model parameters (see declaration *const*) that do not normally change with every call of procedure *LeafC3*. As discussed in the text, these parameters can vary to a certain extent as a function of plant species and/or specific environmental conditions. Thus, they have been declared in a way which allows

programs using this unit to assign new values to them whenever appropriate. The parameters CCgs and CCgb are convergence criteria for g_{sv} and g_{bv}, respectively. They have been assigned default values that optimize both computational speed and numerical accuracy.

```
unit Leaf;
{$N + }
interface

type real = single;
const   Et : real = 81.993328e3;      (* Activation energy for electron transport, J/mol *)
        H : real = 219.81459e3;       (* Enthalpy parameter for electron transport, J/mol *)
        S : real = 711.35712;         (* Enthalpy parameter for electron transport, J mol-1 K-1 *)
        Astom : boolean = True;       (* True = amphystomatous leaf,
                                         False = hypostomatous leaf *)
        Aql : real = 0.85;            (* Leaf absorption coefficient for PPFD *)
        theta : real = 0.8;           (* Coefficient controlling the smoothness of transition between
                                         light- and temperature-limited potential rates of electron transport *)
        Cdr : real = 0.015;           (* Proportionality coefficient for estimating leaf dark respiration *)
        CCgs : real = 200;            (* Convergence criterium for stomatal conductance,
                                         μmol m-2 s-1 *)
        CCgb : real = 4000;           (* Convergence criterium for leaf-boundary layer conductance,
                                         μmol m-2 s-1 *)

procedure LeafC3 (var An,Gs,Gb,Tl,LHeat,Vm25,Jm25,Kc25,Ko25,
f,m,Bs,Dleaf, Dshoot,Pcr,Npw,Plw,Pa,Ca,Oa,Ta,RH,Ri,PPFD,WSpeed, Wstat : real);
implementation

function arcos (var c : double) : double;
(*
        Calculates arccos (in radiant) of the argument c
        (0 <= c <= 1). The function is used for solving
        cubic equations in the model.
*)
var arc : double;
begin
        if c = 0 then arcos := pi*0.5 else
        begin
          arc := arctan(sqrt(1-sqr(c)) / c);
          if c < 0 then arcos := pi + arc else arcos := arc;
        end;
end;

function LBLCond (var Gbf,Grf,Tl,Ta,Tav,Ea,Es,rP,Gs,Wstat : real) : real;
(*
        Estimates leaf-boundary layer conductance (μmol m-2 s-1)
        as the larger of the conductances resulting from forced- and free-convective exchanges.
*)
```

```
begin
        Tlk := Tl + 273.16;
        Ct := Grf*exp(-0.44*ln(Tlk))*sqrt(Tl + 393.16);
        if Wstat <= 0 then begin
            Eb := abs(Tl-Ta);
            if Eb > 1 then Gb := Ct*sqrt(sqrt(Eb*
            (1 + 0.378*rP*Ea)))
                else Gb := 0.2e6;
            n := 0;
            repeat
              Inc(n);
              Gbe := Gb;
              Eb := (Gs*Es + Gbe*Ea) / (Gbe + Gs);
              Eb := Tlk / (1 - 0.378*Eb*rP) - Tav;
              Gb := Ct*sqrt(sqrt(abs(Eb)));
            until (Abs(Gb-Gbe) < CCgb) or (n >= 12);
        end else begin
            Eb := Tlk / (1 - 0.378*Es*rP) - Tav;
            Gb := Ct*sqrt(sqrt(abs(Eb)));
        end;
        if (Gbf >= Gb) then LBLCond := Gbf else LBLCond := Gb;
end;

function LeafTemp (var Ri,Ta,Ea,rPs,HCair,Gs,Gb,Cfm,Wstat,Mbv : real): real;
(*
        Calculates leaf temperature (° C) by solving a quartic form
        of the energy-balance equation.
*)
var he,ht,k,a,sa,b,c,d,Q,P,Dscr,y,R,t1,E : double;
begin
        if Wstat <= 0 then he := rPs*Cfm*Gs*Gb*Mbv / (Gs + Mbv*Gb)
                      else he := rPs*Cfm*Gb;
        ht := HCair*Cfm*(0.924*Gb);
        k := 1 / (1.10565e-7 + he*5.8243608e-4);
        a := k*(1.2080774e-4 + he*1.5841967e-2);
        b := k*(0.049499764 + he*1.5518613);
        c := k*(9.014237 + he*44.513596 + ht);
        d := k*(he*(608.563-Ea) - Ri - ht*Ta + 615.58224);
        y := a*c - 4*d;
        E := sqr(b); sa := sqr(a);
        P := (3*y - E)*0.1111111111;
        Q := (b*(2*E - 9*y) - 27*(d*(4*b-sa)-sqr(c))) / 54;
        Dscr := sqrt(sqr(Q) + P*sqr(P));
        y := exp(ln(Q + Dscr) / 3) - exp(ln(Dscr-Q) / 3) + 0.3333333333*b;
        R := sqrt(0.25*sa + y - b);
        t1 := 0.25*(a*(4*b-sa)-8*c) / R;
        E := 0.5*sa - b - y;
        LeafTemp := -0.25*a - 0.5*(R-sqrt(E-t1));
end;
```

```
function StomCond (var Es,M,Bs,An,Ca,Gb,Tl,Ea,Wstat,Mbv : real) : double;
(*      Calculates leaf stomatal conductance to water vapor (μmol
        m^-2 s^-1) by solving a quadratic equation.
*)
var Cb,a,b,c,MAn,Gs,Gbt : double;
begin
        Es := 610.7*exp(17.38*Tl/(Tl + 239));
        MAn := M*An;
        Gbt := Mbv*Gb;
        Cb := Ca - 1.37*An/Gbt;
        if Wstat <= 0 then begin
            a := Es*Cb;
            b := Es*(MAn - Cb*(Gbt-Bs*1e6));
            c := Gbt*(MAn*Ea + Cb*Es*Bs*1e6);
            Gs := 0.5*(b + sqrt(sqr(b) + 4*a*c))/a;
        end else Gs := MAn/Cb + Bs*1e6;
        if Gs > 0 then StomCond := Gs else StomCond := 0;
end;

function C3NetAssim (var Pa,Cap,Oa,PPFD,Is,Gs,Gb,Tl,Kc25,Ko25,Jm25,
Vm25,Mbv : real) : real;
(*
        Calculates leaf net photosynthesis rate (μmol m^-2 s^-1)
        by solving a quartic equation.
*)
var Km,Ccp,Vcm,Jcm,J,R,a,sa,b,c,d,L,alfa,gm,Rt,sRt,N,Q,P,W,t1 :
double; Wc,Wj,Rd,Agr : real;
begin
        N := Tl + 273.16;
        Q := Tl - 25;
        Ccp := Pa*Oa*(213.88e-6 + Q*(8.995e-6 + 1.722e-7*Q));
        R := 0.12027905/N;
        Km := Pa*Kc25*exp(32.462 - 80470*R);
        Vcm := Vm25*exp(46.9411 - 116300*R)/
        (1 + exp((650*N - 202900)*R));
        if PPFD < 50 then L := PPFD*0.01332 else L := 0.666;
        Rd := Cdr*Vm25*(1.666 - L)*exp(34.07 - 84450*R);
        if Tl > 52 then Rd := Rd/(1 + exp(1.3*(Tl-56)));
        Jcm := Jm25*exp((N*3.362135e-3 - 1)*Et*R)/
        (1 + exp((S*N -H)*R));
        J := 0.111111*(Jcm + Is - Sqrt(sqr(Jcm + Is)
        - 4*theta*Jcm*Is))/theta;
        if Gs > 0 then begin
                                Rt := Pa*(1.6*Mbv*Gb + 1.37*Gs)/(Mbv*Gs*Gb);
                                sRt := sqr(Rt);
                                Km := Km*(1 + Oa/(Ko25*exp(5.854 - 14510/(8.314*N))));
                                N := (2.33*Ccp + Km);
                                P := Vcm + J;
```

```
                W := Vcm*J;
                Q := 1.33*Vcm*Ccp + J*(Km - Ccp);
                L := Ccp*(2.33*Vcm*Ccp + J*Km);
                alfa := 0.97*(Cap*(Cap + N) + 2.33*Ccp*Km);
                gm := 1/(0.97*sRt);
                R := 0.97*(2*Cap + N);
                a := gm*(sRt*(2*0.97*Rd - P) - Rt*R);
                b := gm*(alfa + Rt*(Rd*(Rt*(0.97*Rd - P) - 2*R)
                + 2*P*Cap + Q + W*Rt));
                c := gm*(Rd*(2*alfa + Rt*(2*P*Cap + Q - Rd*R))
                -Cap*(P*Cap + Q) + L - 2*W*Rt*(Cap - Ccp));
                d := gm*(Rd*(Rd*alfa - Cap*(P*Cap + Q) + L)
                + W*(Cap*(Cap - 2*Ccp) + sqr(Ccp)));
                sa := sqr(a); gm := a*c - 4*d; L := sqr(b);
                P := abs((3*gm - L))*0.1111111111;
                W := sqrt(P);
                Q := (b*(2*L-9*gm) - 27*(d*(4*b-sa)-sqr(c)))/54;
                t1 := Q/(P*W);
                t1 := arcos(t1)*0.3333333333;
                N := 2*W*cos(t1) + 0.3333333333*b;
                R := sqrt(0.25*sa + N - b);
                L := sqrt(0.5*sa - b - N - 0.25*(a*(4*b-sa)-8*c)/R);
                Agr := -0.25*a - 0.5*(R + L) + Rd;
                Wc := 0.5*Vcm;
                Agr := 0.5263*(Agr + Wc - sqrt(sqr(Agr + Wc) - 3.8*Agr*Wc));
        end else Agr := 0;
        C3NetAssim := Agr - Rd;
end;

procedure LeafC3;
(*
        The main program of the LEAFC3 model.
*)
var Mt,LHV,rPs,Cfm,G,Ea,Bsc,Es,dGb,Gbf,Grf,rP, VHCair,Gbc,Mbv,Tav,
Is,Cap,Ria : real;
        n : byte;
begin
        Cap := Pa*Ca;
        Ea := RH*6.107*exp(17.38*Ta/(Ta + 239));
        rP := 1/Pa;
        Tav := Ta + 273.16;
        Cfm := 8.3089764e-6*Tav*rP;
        LHV := (2.50084 - 0.00234*Ta)*1e6;
        rPs := 2.1669236e-3*LHV/Tav;
        VHCair := 3.518638*Pa/Tav;
        if PPFD < 100 then Bsc := Bs*(PPFD*0.009 + 0.1)
        else Bsc := Bs;
        Is := 0.5*Aql*(1-f)*PPFD;
```

```
        if Plw <> 0 then Mt := m / (1 + exp(Npw * ln(Plw / Pcr)))
        else Mt := m;
        Gbf := exp(-0.44 * ln(Tav)) * sqrt((Ta + 393.16)
        * WSpeed * Pa / Dleaf);
        if (Dshoot > 0) and (Dleaf <= 6e-3) then begin
            Gbf := 144.84335 * Gbf;
            Grf := 104.33295 * sqrt(Pa / sqrt(Dshoot));
            Mbv := 1;
        end else begin
            Gbf := 520.16034 * Gbf;
            Grf := 196.90753 * sqrt(Pa / sqrt(Dleaf));
            if Astom then Mbv := 1 else Mbv := 0.5;
        end;
        if WSpeed <= 0.28 then Tav := Tav / (1 - 0.378 * Ea * rP);
        if Gbf > 0.2e6 then Gb := Gbf else Gb := 0.2e6;
        if PPFD > 0 then
                                    Gs := (PPFD / (PPFD + 65)) * 0.0015 * Vm25 * exp(0.07 * (Ta-25))
                                    * Mt * RH / Ca + Bsc * 1e6
        else Gs := 0.5e6 * Bsc;
        n := 0; Tl := Ta;
        dGb := 0; Ria := Ri;
        repeat
            Inc(n);
            G := Gs;
            if WSpeed <= 0.28 then begin
              Gbc := LBLCond (Gbf,Grf,Tl,Ta,Tav,Ea,Es,
              rP,Gs,Wstat);
              dGb := Gb - Gbc; Gb := Gbc;
            end;
            Tl := LeafTemp (Ria,Ta,Ea,rPs,VHCair,G,Gb,Cfm,Wstat,Mbv);
            An := C3NetAssim (Pa,Cap,Oa,PPFD,Is,G,Gb,Tl,Kc25,Ko25,
            Jm25,Vm25,Mbv);
            Gs := StomCond (Es,Mt,Bsc,An,Ca,Gb,Tl,Ea,Wstat,Mbv);
            Ria := Ri - 0.506 * An;
        until ((Abs(Gs-G) < CCgs) and (Abs(dGb) < CCgb)) or (n > 40);
        LHeat := rPs * (Es - Ea) * Cfm * Gb;
        if Wstat <= 0 then LHeat := LHeat * Gs * Mbv / (Gs + Mbv * Gb);
end;

end. (* End of Unit Leaf *)
```

References

Amthor, J.S., Koch, G.W. and Bloom, A.J., 1992. CO_2 inhibits respiration in leaves of *Rumex crispus* L. Plant Physiol., 98: 757–760.

Aphalo, P.J. and Jarvis, P.G., 1993a. An analysis of Ball's empirical model of stomatal conductance. Ann. Bot., 72: 321–327.

Aphalo, P.J. and Jarvis, P.G., 1993b. The boundary layer and the apparent responses of stomatal conductance to wind speed and to the mole fractions of CO_2 and water vapor in the air. Plant Cell Environ., 16: 771–783.

Aphalo, P.J. and Jarvis, P.G., 1991. Do stomata respond to relative humidity? Plant Cell Environ., 14: 127–132.

Avissar, R. and Pielke, R.A., 1991. The impact of plant stomatal control on mesoscale atmospheric circulations. Agric. For. Meteorol., 54: 353–372.

Azcon-Bieto, J., Farquhar, G.D. and Caballero, A., 1981. Effects of temperature, oxygen concentration, leaf age and seasonal variation on the CO_2 compensation point in *Lolium perenne* L.: comparison with a mathematical model including non-photorespiratory CO_2 production in the light. Planta, 152: 497–504.

Baldocchi, D.D., 1993. Scaling water vapor and carbon dioxide exchange from leaves to a canopy: rules and tools. In: J.R. Ehleringer and C.B. Field (Editors), Scaling Physiological Processes: Leaf to Globe. Academic Press, San Diego, CA, pp. 77–116.

Baldocchi, D.D., Verma, S.B. and Anderson, D.E., 1987. Canopy photosynthesis and water-use efficiency in a deciduous forest. J. Appl. Ecol., 24: 251–260.

Ball, J.T., 1988. An analysis of stomatal conductance. Ph.D. thesis, Stanford University, CA, 89 pp.

Ball, J.T., 1987. Calculations related to gas exchange. In: E. Zeiger, G.D. Farquhar and I.R. Cowan (Editors), Stomatal Function. Stanford University Press, Stanford, CA, pp. 445–476.

Ball, J.T., Woodrow, I.E. and Berry, J.A., 1987. A model predicting stomatal conductance and its contribution to the control of photosynthesis under different environmental conditions. In: J. Biggens (Editor), Progress in Photosynthesis Research, Vol. IV. Martinus Nijhoff Publishers, Dordrecht, pp. 221–224.

Beadle, C.L., Jarvis, P.G. and Neilson, R.E., 1979. Leaf conductance as related to xylem water potential and carbon dioxide concentration in Sitka spruce. Physiol. Plant., 45: 158–166.

Berry, J. and Björkmann, O., 1980. Photosynthetic response and adaptation to temperature in higher plants. Annu. Rev. Plant Physiol., 31: 491–543.

Besford, R.T., 1990. The greenhouse effect: Acclimation of tomato plants growing in high CO_2, relative change in Calvin cycle enzymes. J. Plant Physiol., 136: 458–463

Brooks, A. and Farquhar, G.D., 1985. Effects of temperature on the CO_2/O_2 specificity of ribulose-1,5-bisphosphate carboxylase/oxygenase and the rate of respiration in the light. Planta, 165: 397–406.

Bunce, J.A., 1985. Effects of boundary layer conductance on the response of stomata to humidity. Plant Cell Environ., 8: 55–57.

Campbell, G.S., 1977. An Introduction to Environmental Biophysics. Springer-Verlag, New York, 155 pp.

Collatz, G.J., Ball, J.T., Grivet, C. and Berry, J.A., 1991. Physiological and environmental regulation of stomatal conductance, photosynthesis and transpiration: a model that includes a laminar boundary layer. Agric. For. Meteorol., 54: 107–136.

Delucia, E., Sasek, T. and Strain, B., 1985. Photosynthetic inhibition after long-term exposure to elevated levels of atmospheric carbon dioxide. Photosynth. Res., 7: 175–184.

Deng, X., Joly, R.J. and Hahn, D.T., 1990. The influence of plant water deficit on photosynthesis and translocation of ^{14}C-labeled assimilates in cacao seedlings. Physiol. Plant., 78: 623–627.

Dixon, M. and Grace, J., 1984. The effect of wind on the respiration of young trees. Ann. Bot., 53: 811–819.

Dougherty, R.L., Bradford, J.A., Coyne, P.I. and Sims, P.L., 1994. Applying an empirical model of stomatal conductance to three C-4 grasses. Agric. For. Meteorol., 67: 269–290.

Eamus, D. and Jarvis, P.G., 1989. The direct effect of increase in the global atmospheric CO_2 concentration an natural and commercial temperate trees and forests. Adv. Ecol. Res., 19: 1–55.

Evans, J.R., 1989. Partitioning of nitrogen between and within leaves grown under different irradiances. Aust. J. Plant Physiol., 16: 533–548.

Farquhar, G.D., 1988. Models relating subcellular effects of temperature to whole plant responses. In: S.P. Long and F.I. Woodward (Editors), Plants and Temperature. Society for Experimental Biology, University of Cambridge, Cambridge, pp. 395–409.

Farquhar, G.D. and von Caemmerer, S., 1982. Modelling of photosynthetic response to environmental conditions. In: O.L. Lange, P.S. Nobel, C.B. Osmond and H. Ziegler (Editors), Physiological Plant Ecology II. Water Relations and Carbon Assimilation. Springer-Verlag, Berlin, pp. 549–587.

Farquhar, G.D. and Wong, S.C., 1984. An empirical model of stomatal conductance. Aust. J. Plant Physiol., 11: 191–210.

Farquhar, G.D., von Caemmerer, S. and Berry, J.A., 1980. A biochemical model of photosynthetic CO_2 assimilation in leaves of C_3 species. Planta 149: 78–90.

Fields, C., 1983. Allocating leaf nitrogen for maximization of carbon gain: leaf age as a control on the allocation program. Oecologia, 56: 341–347.

Fisher, M.J., Charles-Edwards, D.A. and Ludlow, M.M., 1981. An analysis of the effects of repeated short-term soil water deficits on stomatal conductance to carbon dioxide and leaf photosynthesis by legume *Macroptilium atropurpureum* cv. Siratro. Aust. J. Plant Physiol., 8: 347–357.

Friend, A.D., 1991. Use of a model of photosynthesis and leaf microenvironment to predict optimal stomatal conductance and leaf nitrogen partitioning. Plant Cell Environ., 14: 895–905.

Gates, D.M., 1980. Biophysical Ecology. Springer-Verlag, New York, 611 pp.

Givnish, T.J., 1986. Optimal stomatal conductance, allocation of energy between leaves and roots, and the marginal costs of transpiration. In: T.J. Givnish (Editor), On the Economy of Plant Form and Function. Cambridge University Press, Cambridge, pp. 171–213.

Grace, J., Malcolm, D.C. and Bradbury, I.K., 1975. The effect of wind and humidity on leaf diffusive resistance in Sitka spruce seedlings. J. Appl. Ecol., 12: 931–940.

Grant, R.H., 1984. The mutual interference of spruce canopy structural elements. Agric. For. Meteorol., 32: 145–156.

Grantz, D.A., 1990. Plant response to atmospheric humidity. Plant Cell Environ., 13: 667–679.

Gueymard, C., 1993. Assessment of the accuracy and computing speed of simplified saturation vapor equations using a new reference dataset. J. Appl. Meteorol., 32: 1294–1300.

Harley, P.C. and Tenhunen, J.D., 1991. Modeling the photosynthetic response of C_3 leaves to environmental factors. In: K.J. Boote and R.S. Loomis (Editors), Modeling Crop Photosynthesis – From Biochemistry to Canopy. CSSA Special Publication no. 19. American Society of Agronomy and Crop Science Society of America, pp. 17–39.

Harley, P.C., Thomas, R.B., Reynolds, J.F. and Strain, B.R., 1992. Modelling photosynthesis of cotton grown in elevated CO_2. Plant Cell Environ., 15: 271–282.

Hinckley, T.M., Lassoie, J.P. and Running, S.W., 1978. Temporal and spatial variations in the water status of forest trees. For. Sci. Monogr., 20: 1–72.

Hinckley, T.M., Duhme, F., Hinckley, A.R. and Ritcher, H., 1983. Drought relations of shrub species: Assessment of the mechanisms of drought resistance. Oecologia, 59: 344–350.

Idso, S.B. and Kimball, B.A., 1993. Effects of atmospheric CO_2 enrichment on net photosynthesis and dark respiration rates of three Australian tree species. J. Plant Physiol., 141: 166–171.

Idso, S.B., Kimball, B.A., Anderson, M.G. and Mauney, J.K., 1987. Effects of atmospheric CO_2 enrichment on plant growth: the interactive role of air temperature. Agric. Ecosyst. Environ., 20: 1–10.

Jarvis, P.G., 1976. The interpretation of the variations of leaf water potential and stomatal conductance found in canopies in the field. Phil. Trans. R. Soc. London B, 273: 593–610.

Kaufmann, M.R., 1981. Automatic determination of conductance, transpiration, and environmental conditions in forest trees. For. Sci., 27: 817–827.

Kaufmann, M.R., 1982a. Leaf conductance as a function of photosynthetic photon flux density and absolute humidity difference from leaf to air. Plant Physiol., 69: 1018–1022.

Kaufmann, M.R., 1982b. Evaluation of season, temperature, and water stess effects on stomata using a leaf conductance model. Plant Physiol., 69: 1023–1026.

Kent, S.S., Andre, A., Cournac, L. and Farineau, J., 1992. An integrated model for the determination of the Rubisco specificity factor, respiration in the light and other photosynthetic parameters of C_3 plants in situ. Plant Physiol. Biochem., 30: 625–637.

Kimball, B.A., 1985. Adaptation of vegetation and management practices to a higher carbon dioxide world. In: B.R. Strain and J.D. Cure (Editors), Direct Effect of Increasing Carbon Dioxide on Vegetation. DOE/ER-0238, US Department of Energy, Washington, DC, pp. 185–204.

Knapp, A.K., 1993. Gas exchange dynamics in C_3 and C_4 grases: Consequences of differences in stomatal conductance. Ecology, 74: 113–123.

Knapp, A.K. and Smith, W.K., 1989. Influence of growth form on ecophysiological responses to variable sunlight in subalpine plants. Ecology, 70: 1069–1082.

Knapp, A.K. and Smith, W.K., 1990. Stomatal and photosynthetic responses to variable sunlight. Physiol. Plant., 78: 160–165.

Landsberg, J.J., 1986. Physiological Ecology of Forest Production. Academic Press, London, 198 pp.

Lemon, E.R. (Editor), 1983. CO_2 and Plants: The Response of Plants to Rising Levels of Atmospheric Carbon Dioxide. Westview Press, Boulder, CO.

Leuning, R., 1990. Modelling stomatal behavior and photosynthesis in *Eucalyptus grandis*. Aust. J. Plant Physiol., 17: 159–175.

Leuning, R., Cromer, R.N. and Rance, S., 1991. Spatial distributions of foliar nitrogen and phosphorus in crowns of *Eucalyptus grandis*. Oecologia, 88: 504–510.

Lloyd, J., 1991. Modelling stomatal responses to environment in *Macadamia integrifolia*. Aust. J. Plant Physiol., 18: 649–660.

Massman, W.J. and Kaufmann, M.R., 1991. Stomatal response to certain environmental factors: a comparison of models for subalpine trees in the Rocky Mountains. Agric. For. Meteorol.,54: 155–167.

Monteith, J.L. and Unsworth, M.H., 1990. Principles of Environmental Physics. Edward Arnold, London, 291 pp.

Norman, J.M., 1993. Scaling processes between leaf and canopy levels. In: J.R. Ehleringer and C.B. Field (Editors), Scaling Physiological Processes: Leaf to Globe. Academic Press, San Diego, CA, pp. 41–76.

Oechel, W.C. and Strain, B.R., 1985. Native species responses to increased atmospheric carbon diodide concentration. In: B.R. Strain and J.D. Cure (Editors), Direct Effect of Increasing Carbon Dioxide on Vegetation. DOE/ER-0238, U.S. Department of Energy, Washington, DC, pp. 118–154.

Osonubi, O. and Davies, W.J., 1980. The influence of water stress on the photosynthetic performance and stomatal behavior of tree seedlings subjected to variation in temperature and irradiance. Oecologia, 45: 3–10.

Paw U, K.T., 1987. Mathematical analysis of the operative temperature and energy budget. J. Thermal Biol., 3: 227–233.

Peisker, M., Ticha, I. and Čatsky, J., 1981. Ontogenic changes

in the internal limitations to bean-leaf photosynthesis. 7. Interpretations of the linear correlation between CO_2 compensation concentration and CO_2 evolution in darkness. Photosynthetica (Prague), 15: 161–168.

Pielke, R.A., Schimel, D.S., Lee, T.J., Kittel, T.G.F. and Zeng, X., 1993. Atmosphere-terrestrial ecosystem interactions: implications for coupled modeling. Ecol. Model., 67: 5–18.

Rawson, H.M., 1992. Plant responses to temperature under conditions of elevated CO_2. Aust. J. Bot., 40: 473–490.

Schoettle, A.W., 1990. Importance of shoot structure to sunlight interception and photosynthetic carbon gain in *Pinus contorta* crowns. Ph.D. thesis, University of Wyoming, 200 pp.

Sharkey, T.D., 1985a. Photosynthesis in intact leaves of C_3 plants: physics, physiology and rate limitations. Bot. Rev., 51: 53–105.

Sharkey, T.D., 1985b. O_2-Insensitive photosynthesis in C_3 plants: its occurrence and a possible explanation. Plant Physiol., 78: 71–75.

Sharp, R.E., Matthews, M.A. and Boyer, J.S., 1984. Kok effect and the quantum yield of photosynthesis: light partially inhibits dark respiration. Plant Physiol., 75: 95–101.

Sinclair, T.R., Tanner, C.B. and Bennett, J.M., 1984. Water-use efficiency in crop production. BioScience, 34: 36–40.

Smolander, H., Oker-Blom, P., Ross, J., Kellomaki, S. and Lahti, S., 1987. Photosynthesis of a scotch pine shoot: test of a shoot photosynthesis model in a direct radiation field. Agric. For. Meteorol., 39: 67–80.

Tanner, C.B. and Sinclair, T.R., 1983. Efficient water use in crop production. In: H.M. Taylor, W.R. Jordan and T.R. Sinclair (Editors), Limitations to Efficient Water Use in Crop Production, American Society of Agronomy, Madison, WI, pp. 1–27.

Thompson, W.A. and Wheeler, A.M., 1992. Photosynthesis by mature needles of field-grown *Pinus radiata*. For. Ecol. Manage., 52: 225–242.

Verstraete, M.M., 1985. A soil–vegetation–atmosphere model for micrometeorological research in arid regions. Cooperative Thesis No. 88, Massachusetts Institute of Technology and National Center for Atmospheric Research, Boulder, CO.

Von Caemmerer, S. and Farquhar, G.D., 1981. Some relationships between biochemistry of photosynthesis and the gas exchange of leaves. Planta, 153: 376–387.

Waring, R.H. and Schlesinger, W.H., 1985. Forest Ecosystems. Concepts and Management. Academic Press, Orlando, 340 pp.

Wong, S.C., Cowan, I.R. and Farquhar, G.D., 1985a. Leaf conductance in relation to rate of CO_2 assimilation. I. Influence of nitrogen nutrition, phosphorous nutrition, photon flux density and ambient partial pressure of CO_2 during ontogeny. Plant Physiol., 78: 821–825.

Wong, S.C., Cowan, I.R. and Farquhar, G.D., 1985b. Leaf conductance in relation to rate of CO_2 assimilation. III. Influence of water stress and photoinhibition. Plant Physiol., 78: 830–834.

Woodrow, I.E. and Berry, J.A., 1988. Enzymatic regulation of photosynthetic CO_2 fixation in C_3 plants. Annu. Rev. Plant Mol. Biol., 39: 533–594.

Wullschleger, S.D. and Norby, R.J., 1992. Respiratory cost of leaf growth and maintenance in white oak saplings exposed to atmospheric CO_2 enrichment. Can. J. For. Res., 22: 1717–1721.

Zeiger, E., Farquhar, G.D. and Cowan, I.R., 1987 (Editors). Stomatal Function. Stanford University Press, Stanford, CA, 503 pp.

Ziegler-Jöns, A. and Selinger, H., 1987. Calculation of leaf photosynthetic parameters from light-response curves for ecophysiological applications. Planta, 171: 412–415.

Zur, B. and Jones, J.M., 1984. Diurnal changes in the instantaneous water-use efficiency of a soybean crop. Agric. For. Meteorol., 33: 41–51.